

Artificial Molecular Motors

DOI:

[10.1039/C7CS00245A](https://doi.org/10.1039/C7CS00245A)

Document Version

Accepted author manuscript

[Link to publication record in Manchester Research Explorer](#)

Citation for published version (APA):

Kassem, S., van Leeuwen, T., Lubbe, A. S., Wilson, M., & Feringa, B. L. (2017). Artificial Molecular Motors. *Chemical Society Reviews*, 46, 2592-2621. <https://doi.org/10.1039/C7CS00245A>

Published in:

Chemical Society Reviews

Citing this paper

Please note that where the full-text provided on Manchester Research Explorer is the Author Accepted Manuscript or Proof version this may differ from the final Published version. If citing, it is advised that you check and use the publisher's definitive version.

General rights

Copyright and moral rights for the publications made accessible in the Research Explorer are retained by the authors and/or other copyright owners and it is a condition of accessing publications that users recognise and abide by the legal requirements associated with these rights.

Takedown policy

If you believe that this document breaches copyright please refer to the University of Manchester's Takedown Procedures [<http://man.ac.uk/04Y6Bo>] or contact uml.scholarlycommunications@manchester.ac.uk providing relevant details, so we can investigate your claim.





Artificial Molecular Motors

Salma Kassem,^{a†} Thomas van Leeuwen,^{b†} Anouk S. Lubbe,^{b†} Miriam R. Wilson,^{a†} Ben L. Feringa,^{b*} David A. Leigh^{a*}

Received 00th January 20xx,
Accepted 00th January 20xx

DOI: 10.1039/x0xx00000x

www.rsc.org/

Motor proteins are nature's solution for directing movement at the molecular level. The field of artificial molecular motors takes inspiration from these tiny but powerful machines. Although directional motion on the nanoscale performed by synthetic molecular machines is a relatively new development, significant advances have been made. In this review an overview is given of the principal designs of artificial molecular motors and their modes of operation. Although synthetic molecular motors have also found widespread application as (multistate) switches, we focus on the control of directional movement, both at the molecular scale and at larger magnitudes. We identify some key challenges remaining in the field.

1. Introduction

The living cell is a miniscule factory filled with an array of motor proteins tasked with carrying out key biological processes.^{1–3} Over the last few decades much effort has been invested into understanding their modes of action.^{4–9} Most protein-based motors utilize, directly or indirectly, energy derived from adenosine triphosphate (ATP) hydrolysis.^{5,6,10,11} Other energy sources for molecular level processes include trans-membrane ionic gradients, which fuel the synthesis of ATP and most ionic transport processes, and sunlight, which provides the energy for photosynthesis.^{2,3} Insights from biological molecular motors has enabled synthetic chemists to understand the basic requirements needed to design artificial molecular motors and the different mechanisms by which they can operate. A number of synthetic molecular machines that enable controlled movement of molecular components have been developed.^{12–18} Some take inspiration from macroscopic machines (brakes,¹² elevators,¹³ nanocars,¹⁵ shuttles^{16,17} etc.), while others feature ratchet mechanisms^{18–21} and/or mimic biological counterparts (molecular synthesisers,^{22,23} transporters²⁴ and walkers^{25,26,27,43}).

In this review we highlight the recent developments on translational and rotational motors and illustrate how molecular motors can be harnessed to achieve function. For other discussions on this topic, either on earlier work or with a different focus, we refer to the reviews by some of the main contributors to the field of molecular motors.^{7,27,43}

1.1. Terminology of machines, switches, motors and ratchets

In order to discuss the development of small-molecule motors, the terms 'machine', 'switch' and 'motor' need to be defined in molecular terms. The use of those terms in this Review are consistent with their use in physics and biology.^{27,18,27e,43} A 'molecular machine' is a system in which a stimulus triggers the controlled motion of one molecular or submolecular component relative to another, potentially resulting in a net task being performed.¹⁸ A 'molecular switch' is a type of molecular machine in which the change in relative positions of the components influences a system as a function of the state of the switch. (A consequence of this that when a switch is returned to its original state, any mechanical work performed by the original switching action will be undone.) A 'molecular motor' is a molecular machine in which the change in relative position of the components influences a system as a function of the trajectory of the components. When a molecular motor returns to its original state at the end of the motor cycle, the work performed is not undone. The distinction between 'switch' and 'motor' is important; a molecular switch cannot be used to progressively perform work in the way that motors can, unless the switch is part of a larger ratchet (i.e. motor) mechanism.^{27e,43} Only molecular motors can be used to progressively drive systems away from equilibrium.

Machines need to be designed according to their intended operation environment. Molecular machines operate in conditions where gravity and inertia are irrelevant, and viscous forces and Brownian motion dominate - Astumian has noted that molecular machines must "*swim in molasses and walk in a hurricane*".²⁸ The challenge of designing molecular motors lies not with producing motion at the molecular level, but in controlling the directionality of movement.

^a School of Chemistry, University of Manchester, Oxford Road, Manchester, M13 9PL, UK. E-mail: david.leigh@manchester.ac.uk

^b Stratingh Institute for Chemistry, University of Groningen, Nijenborgh 4, 9747 AG Groningen, The Netherlands. E-mail: b.l.feringa@rug.nl

† These authors contributed equally.

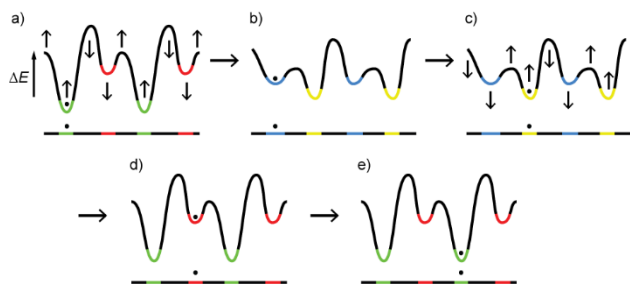


Figure 1: An energy ratchet (flashing ratchet). In (a) and (c) the particle starts in a green or orange well respectively. Raising this energy minima while simultaneously lowering the adjacent energy maxima provides the driving force for the particle to move position by Brownian motion. By repeatedly varying the energy barriers in this way the particle can be directionally transported.^{27e} Adapted from Ref. 27e with permission from the ACS, copyright 2015.

Molecular motors exploit random thermal fluctuations to produce directed motion by employing ratchet mechanisms.^{18,27e,28,43} Brownian ratchets are an essential feature of any machine more sophisticated than a simple switch and fall into two distinct classes: energy ratchets¹⁸ and information ratchets¹⁹.

In its minimalist form an energy ratchet consists of a periodic series of pairs of energy maxima and minima (Figure 1). The particle starts in a green or yellow well (Figure 1, a or c respectively). Raising that energy minima while simultaneously lowering the adjacent minima provides the thermodynamic driving force for the particle to move position by Brownian motion (Figure 1, b to c or d to e). Synchronising the change in the relative heights of the maxima (which determine the direction in which transport proceeds) with the change in the relative depths of the minima (which provide the driving force for directional transport) displaces the particle in a particular direction. Note that the modulation of the energy surface occurs irrespective of the particle's position.

In an information ratchet the position of the particle does impact the potential energy surface. Directional transport is achieved by selectively lowering kinetic barriers to transport in front of the particle, or by selectively raising barriers to transport behind the particle (Figure 2). This requires information to be transferred between the particle and the potential energy surface.

In this review we outline and discuss synthetic small-molecule motors, grouping systems based on the type of motion they perform (translational or rotary) and their structure (non-interlocked and interlocked). We conclude by considering the challenges remaining and future outlooks for the field.

2. Translational Motion

2.1 Synthetic Small-Molecule Walkers

In order to achieve linear directional transport at the molecular level, chemists have designed small-molecule mimics of motor proteins from the dynein, kinesin and myosin

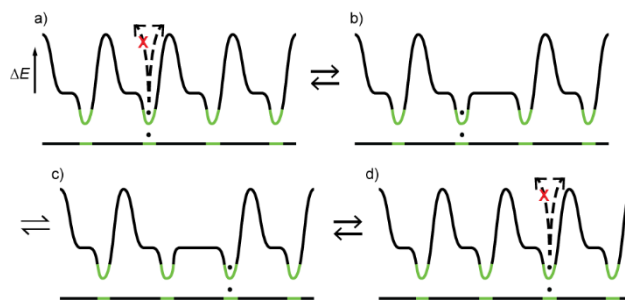


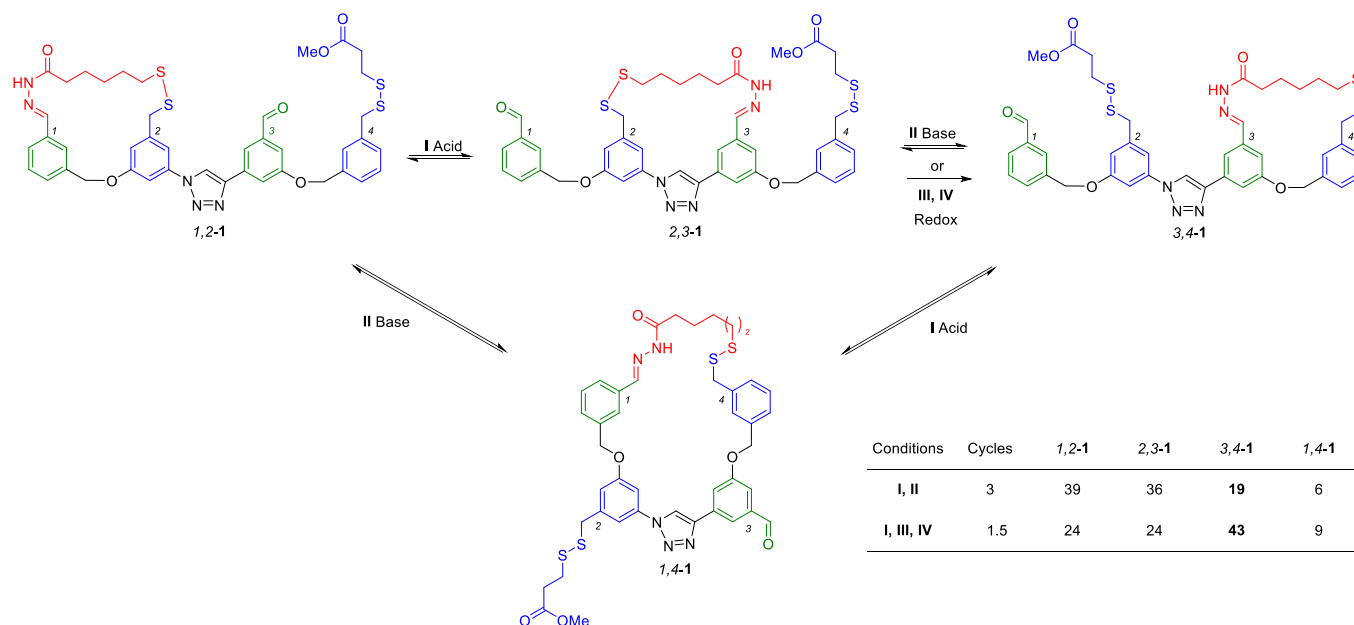
Figure 2: An information ratchet. In (a) and (d) the dashed lines indicate transfer of information about the location of the particle. (b) The position of the particle selectively lowers the energy maxima to the right, but not to the left. (c) The particle moves by Brownian motion.^{27e} Adapted from Ref. 27e with permission from the ACS, copyright 2015.

families that can walk along tracks. Such 'molecular walkers' must fulfil specific requirements for their dynamics:²⁵

- (i) *Processivity*: the molecular walker needs to remain attached to the track during the operation cycle, meaning there should be at least one contact point with the track at all times.
- (ii) *Directionality*: the walker should migrate preferentially or exclusively towards one end of the track.
- (iii) *Repetitive operation*: the walker should be able to repetitively perform cycles of similar mechanical tasks.
- (iv) *Progressive operation*: the walker should return to its original state at the end of a mechanical cycle without returning to its original position or undoing any physical work that has been done.
- (v) *Autonomous operation*: ideally, the walker should continually take 'steps' as long as a fuel is present, without any external intervention.

Several DNA-based molecular walkers systems have been developed,^{29–40} some of which have been shown to operate directionally^{32–36} and autonomously.^{33–39} Here, we will focus on small-molecule walkers, discussing how manipulation of the thermodynamic minima and kinetic barriers of the systems can lead to the development of linear molecular motors in the form of small-molecule walkers.

The first synthetic small-molecule walker was reported in 2010 by Leigh (Scheme 1).^{41,42} The two-legged molecular walker migrates processively along a four-foothold molecular track through a 'passing-leg' mechanism. Processivity is conferred by combining two orthogonal dynamic covalent chemistries - hydrazone and disulfide exchange - as the walker-track binding interactions. The walker's two 'feet' are chemically different and can form covalent bonds reversibly with the track via hydrazone and disulfide exchange reactions in response to a change in the pH of the medium. Under acidic conditions, the hydrazone foot is labile whereas the disulfide foot is kinetically locked onto the track; under basic conditions, the hydrazone foot is kinetically locked whereas the disulfide foot is labile. The orthogonal kinetic stability of the feet prevents the walker from detaching from the track during the walking process while the labile foot is free to take either zero or one step along the track. The walker (1,2-1) takes its first step after the addition of acid. The labile hydrazone foot has a choice



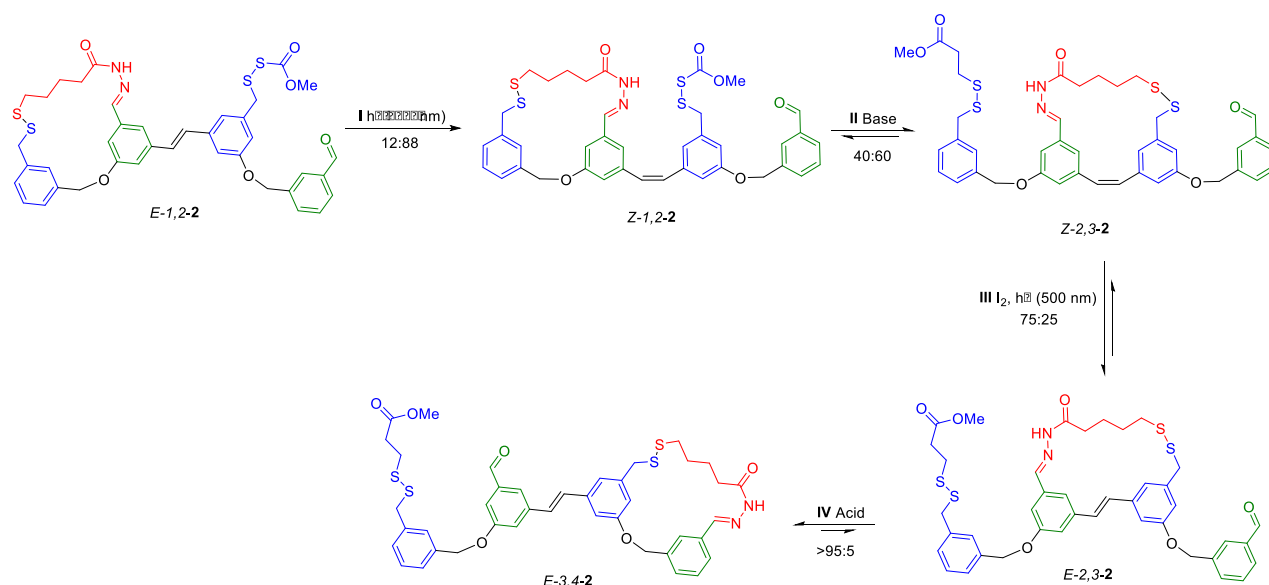
Scheme 1. Design and operation of the first small-molecule walker system by Leigh.⁴¹ Changes in the pH induce the migration of the walker unit (red) from one end of the track to the other by a 'passing-leg' mechanism. The system reaches a steady-state distribution after a few cycles. Replacing the reversible disulfide exchange reaction with a non-reversible redox process results in overall directional transport of the walker away from the minimum-energy distribution.

between two positional isomers accessed by taking zero steps (1,2-1) or taking one step (2,3-1). The two constitutional isomers are in thermodynamic equilibrium under these conditions and there is no preference between them as reflected by the 51:49 distribution of 1,2-1:2,3-1 measured. Addition of base to the mixture labilises the disulfide foot which also has an unbiased choice between zero and one step (3,4-1 from 2,3-1 and 1,4-1 from 1,2-1). The ratio of positional isomers obtained after one cycle (0-2 steps taken by the walker) is 45:36:11:8 for 1,2-1:2,3-1:3,4-1:1,4-1. Both stepping processes are under local thermodynamic control since each positional isomer is in equilibrium with two other isomers under acidic or basic conditions. The steady-state distribution reached after a few cycles of operation is the global minimum energy distribution of the four positional isomers (Scheme 1).

Although the walker migrates from one end of the track to the other under acid-base oscillation, the walking is not inherently directional as the steady-state reached is simply a result of the system relaxing to its minimum energy distribution. In order to confer directionality and drive the walker distribution away from thermodynamic equilibrium, a bias in one of the steps taken by the walker has to be introduced. This could be achieved by replacing the reversible base-promoted disulfide exchange with a two-stage non-reversible redox process. The

reductive ring opening of 2,3-1 generates a tri-thiol which is re-oxidised to reform the disulfide bond to give 2,3-1 or 3,4-1. As the redox process is irreversible, this step is under kinetic control, and results in a different product distribution (after 1.5 cycles 43% of walker molecules have moved to the 3,4 position, compared to 19% after 3 cycles using reversible disulfide exchange, Scheme 1). This behaviour corresponds to an information ratchet mechanism.¹⁹

In a later report, Leigh and co-workers developed a light-driven molecular walker where a more pronounced bias in directionality was achieved through an energy ratchet mechanism (Scheme 2).⁴⁴ Introduction of a stilbene unit between footholds 2 and 3 allows the manipulation of the thermodynamic minima by modifying the ring-strain experienced by the walker. *E*-to-*Z* isomerisation of *E*-1,2-2 produces a 12:88 *E*:*Z* photostationary state. Under disulfide exchange conditions the system equilibrates to 40:60 *Z*-1,2-2:*Z*-2,3-2. Subsequent *Z*-to-*E* isomerisation of the mixture introduces a ring strain in the macrocycle, which, following the addition of acid to promote hydrazone exchange, causes a bias in the stepping process for the non-strained *E*-3,4-2 macrocycle over the strained *E*-2,3-2 (>95:5). This corresponds to an energy ratchet mechanism where the ring strain introduced has altered the thermodynamic minima experienced by the walker at each foothold.



Scheme 2 Design and operation of Leigh's light-driven linear molecular motor system based on a small-molecule walker.⁴⁴ The thermodynamic minima experienced by the walker are manipulated by adjusting the ring-strain between the walker and the track to favour one of two positional isomers.

right transport of the walker (starting from *E*-1,2-2) is achieved by applying the sequence of conditions (I, II, III, IV) with 48% of walker molecules migrating to the 3,4 position, with 30% on the 1,2 position, after one cycle. In a similar manner, 48% of walker units are transported from right-to-left (starting from *E*-3,4-2) through a different order of stimuli application (I, IV, III, II) with 36% remaining on the 3,4 position (Scheme 2). The behaviour of the system was also studied when no stilbene isomerisation steps were performed. Repeatedly alternating between hydrazone and disulfide exchange conditions (thus labilizing one foot then another) allows the walkers on the track to reach the minimum energy distribution. Starting from *E*-1,2-2, the majority of walker units reside equally at each end of the track once the steady-state is reached (7 cycles) with a very small amount of the highly strained *E*-2,3-2 isomer. However, starting from *Z*-1,2-2 the steady state is reached after 2 cycles, as the ring-strain in the three positional isomers (*Z*-1,2-2, *Z*-2,3-2 and *Z*-3,4-2) is comparable and 49% of walker units reside in the central region of the track (*Z*-2,3-2). The differences in the behaviour of the system with and without isomerisation of the stilbene unit demonstrate the effect that the energy ratchet mechanism has on the directionality of this light-driven molecular motor system.

Walker systems **1** and **2** demonstrate how dynamic covalent chemistry can be combined with ratchet mechanisms to directionally transport molecules along tracks. They are the first examples of translational synthetic small-molecule

motors. Other dynamic covalent chemistry-based walkers have been reported^{45–48}. However, in those cases directionality results from the spontaneous downhill migration of the walker towards a thermodynamic sink at one end of the track (i.e. the systems relax towards, rather than are driven away from, a thermodynamic minimum). Recently, small-molecule walkers that feature coordination chemistry for foot-track binding interactions have also been studied.⁴⁹

2.2 Rotaxane-Based Molecular Ratchets

Mechanically interlocking molecular components has some advantages in the operation of small-molecule machines (Figure 3).²⁷ In contrast to molecular walkers, the relative movement of the interlocked components in rotaxanes and catenanes is inherently processive; the components cannot exchange with others in the bulk without breaking covalent bonds. The mechanical bond also restricts the freedom of movement of the components in certain directions, while permitting large-amplitude displacement in other directions (Figure 3).

The template methods used to synthesize mechanically interlocked molecules generally utilise recognition motifs between the components that remain intact after their assembly. The rates of random thermal movement of the components between such sites ('shuttling' between 'stations'), and their degree of occupancy, can often be varied by controlling the strength of the intercomponent interactions.

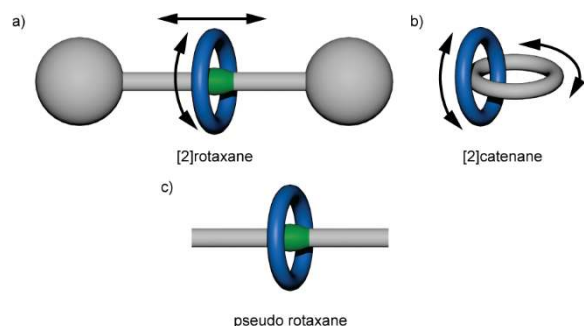


Figure 3. (a) A rotaxane consists of one (or more) axles threaded through one (or more) rings. Bulky groups at each end of the axle prevent the ring from dethreading, but allow the ring to pirouette around the axle and shuttle along it; (b) A catenane is composed of two (or more) macrocycles threaded through each other. The prefix refers to the number of interlocked components. (c) A pseudorotaxane is a supramolecular complex in which a molecule is threaded through the cavity of a macrocycle. The two components are held together by noncovalent bonding interactions but not a mechanical bond.

The first [2]rotaxane ‘molecular shuttle’ **3** was reported by Stoddart’s group and displayed temperature-dependent shuttling of the macrocycle between the two equivalent hydroquinone groups (Figure 4a).¹⁶ Recognition by the authors that ‘Insofar as it becomes possible to control the movement of one molecular component with respect to the other in a [2]rotaxane, the technology for building “molecular machines” will emerge’¹⁶ was a profound observation that essentially started the field of artificial molecular machinery.

The first stimuli-responsive molecular shuttle **4** was also reported by Stoddart group, exploiting variations in pH to switch the preferred position of the macrocycle on the thread between two sites (Figure 4b).⁵⁵ Since then, rotaxane-based switches of various types have been developed by many groups and the relative position of the ring biased through the use of a variety of external stimuli, including redox processes, pH, light, and microenvironment (temperature, solvent, etc.).^{27e}

Although these rotaxane switches have utilised in a variety of tasks, in order to make motors (i.e. machines capable of progressively building on the work done each cycle and to drive systems away from equilibrium) it is necessary to incorporate ratchet mechanisms into the molecular design.

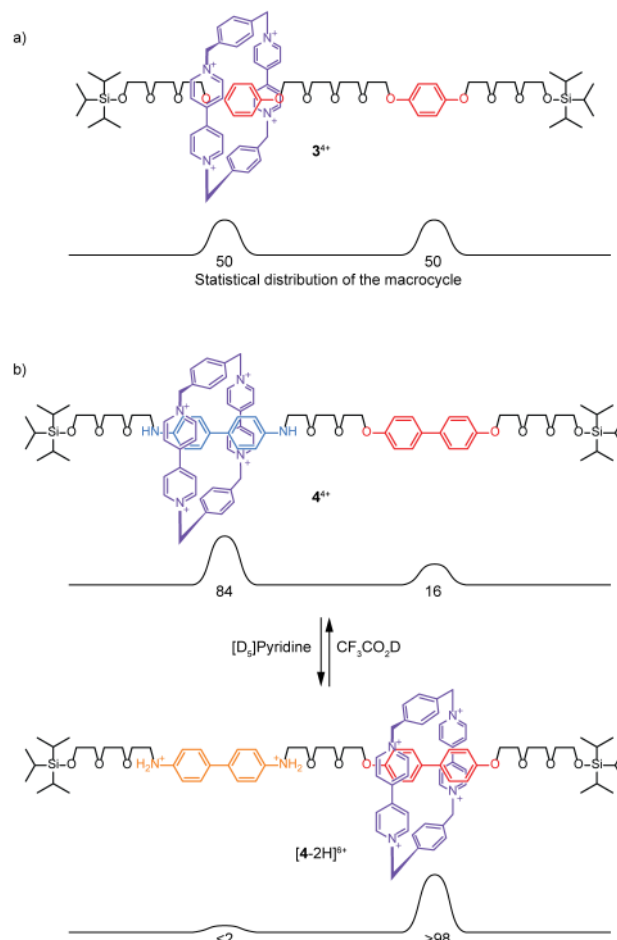


Figure 4 (a) The first molecular shuttle **3** exhibited temperature dependent shuttling between the two degenerate hydroquinone binding sites; (b) Rotaxane switch **4**. At neutral pH the positively charged cyclophane resides over the benzidine station (84:16 distribution), stabilised by π - π stacking. Protonation of the benzidine station creates a driving force for the macrocycle to shuttle to the biphenol site with high positional discrimination (2:98).

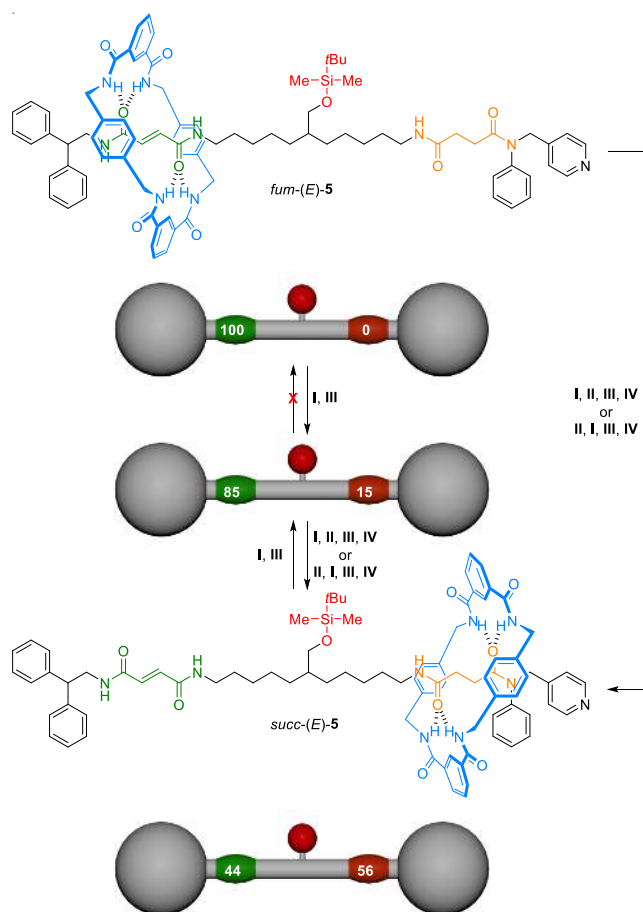


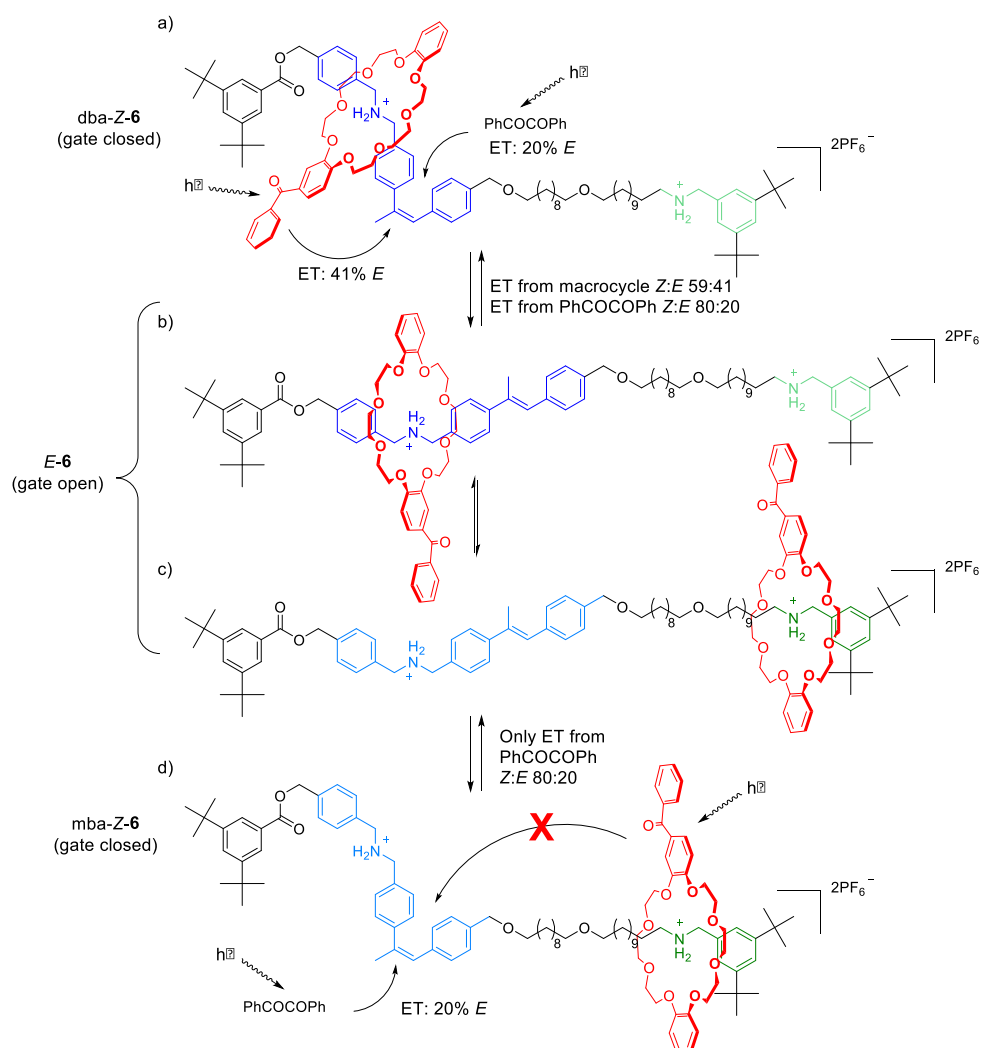
Figure 5. Operation of compartmentalised molecular machine **5**: (I) Desilylation; (II) $E \rightarrow Z$ photoisomerisation; (III) resilylation; (IV) $Z \rightarrow E$ thermal isomerisation. Numbers on the cartoon representations indicate macrocycle distribution.

Rotaxane **5**, developed by the Leigh group, was the first rotaxane to incorporate a ratchet mechanism (Figure 5).¹⁸ It combines the ability to alter relative binding affinities (thermodynamics) with the ability to control exchange between the two stations (kinetics) to create and maintain non-equilibrium macrocycle distributions. The thread of **5** contains fumaramide and succinamide groups separated by a bulky silyl ether, which prevents the macrocycle from shuttling between the two binding sites. The machine can be statistically balanced (85:15 *fum:succ*), and the 'compartments' then unlinked, by simply cleaving and reattaching the silyl blocking group. Next, a balance-breaking stimulus is applied (photoisomerisation at 312 nm, Figure 5, I), which generates a 49:51 $E:Z$ photostationary state. This is followed by removal of the kinetic barrier (linking stimulus, II) which allows balance to be restored through biased Brownian motion of the macrocycle to the new equilibrium distribution. Reinstating the barrier (unlinking stimulus, III) unlinks the compartments, meaning that they are no longer in equilibrium although they remain statistically balanced. The final step (Z -to- E olefin isomerisation, IV) resets the machine, making it statistically unbalanced, unlinked and not in equilibrium.

After one operational cycle 56% of the macrocycles in **5** are positioned on the succinamide station compared to 15% at equilibrium. The ratcheting operation pumps the macrocycle energetically uphill, while returning the thread to its initial state. The mechanism is an energy ratchet.

The first example of a molecular information ratchet was also developed by the Leigh group, in a molecular mimic of the Maxwell Demon thought experiment (Scheme 3).¹⁹ Rotaxane **6** comprises a dibenzo-24-crown-8-based macrocycle mechanically locked onto an axle by bulky 3,5-di-*t*-butylphenyl stoppers. An α -methyl stilbene 'gate' divides the axle into two compartments, each containing an ammonium binding station (dibenzylammonium = blue and monobenzylammonium = green). The macrocycle shuttles randomly along the full length of the thread when the stilbene motif adopts the E conformation *i.e.* the 'gate' is open. However, in the Z conformation, the stilbene motif presents a barrier to translocation, and traps the macrocycle in one or other of the two compartments, *i.e.* the 'gate' is closed. The machine is operated in the presence of an external photosensitiser, PhCOCOPh, to ensure that the gate can close when the macrocycle is on the binding site remote from the stilbene unit. The macrocycle contains a photosensitizer that converts light into the energy necessary to 'open' the gate. Since energy transfer between the macrocycle and gate is distance dependent, the gate opening process is more likely to happen when the macrocycle is located on the blue binding station next to the gate, rather than the green station, where intramolecular energy transfer is inefficient. The operation of the gate is 'information-dependant' since its opening efficiency depends on the position of the macrocycle. The net result of this information transfer is a bias in macrocycle distribution towards the green station, away from the equilibrium value.¹⁸

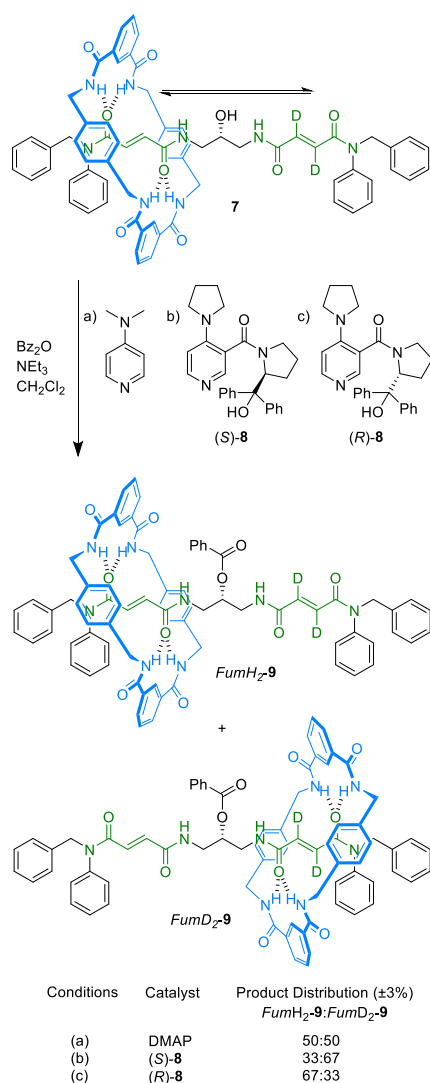
An alternate approach to a molecular information ratchet from Leigh and co-workers exploits another form of chemical information: chirality.²⁰ Rotaxane **7** features a phenyl ester group separated by two fumaramide binding sites (Scheme 4). The close proximity of the stations to the hydroxyl group allows the chiral centre to influence the macrocycle distribution. In the free hydroxyl form the macrocycle is distributed evenly between two fumaramide sites. Acylation of the hydroxyl group of **7** creates a kinetic barrier to shuttling and traps the macrocycle in either compartment. An achiral acylation catalyst DMAP results in an equal distribution of products. However, the chiral DMAP-based acylation catalyst **8** results in an unequal distribution of 33:66 *FumH₂:FumD₂* in favour of the pro-(*S*) fumaramide station (Scheme 4). A reverse in bias was obtained with catalyst (*R*)-**9**. The directional transport results from the ability of the chiral acylation catalyst to use information regarding the position of the macrocycle to preferentially raise the kinetic barrier to shuttling behind the macrocycle. It is effectively a kinetic resolution, with the shuttling of the macrocycle between the two fumaramide sites interconverting two enantiomers.



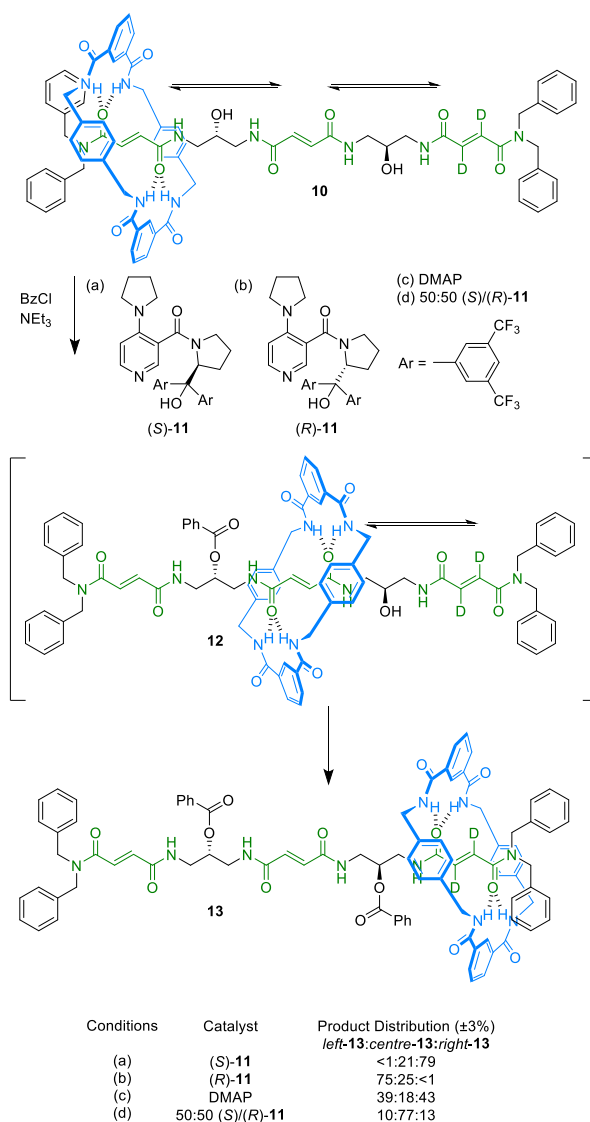
Scheme 3 Molecular information ratchet 6: (a) The stilbene gate is closed, but energy transfer (ET) from the macrocycle is efficient; (b) and (c) the gate is open and the macrocycle is free to shuttle then length of the thread; (d) the macrocycle resides on the green station and intramolecular ET from the macrocycle is inefficient. Intermolecular ET from PhCOCOPh dominates, closing the gate.

A similar ratchet mechanism was applied to a rotaxane with three compartments, allowing cumulative directional pumping of the macrocycle (Scheme 5).²¹ Rotaxane **10** consists of three compartments each containing a fumaramide station separated by hydroxyl groups (Scheme 5). Benzoylation of the hydroxyl groups in the presence of chiral acylation catalyst (*S*)-**11** results in efficient pumping of the macrocycle to the right-hand compartment in a <1:21:79 distribution. The bias is reversed when using catalyst (*R*)-**11**, now favouring a 75:25:<1 macrocycle distribution. When both catalysts are employed simultaneously the macrocycle is trapped in the central compartment in a 10:77:13 distribution. As with the two-

compartment chiral information ratchet (Scheme 4), the mechanism of the three-compartment information ratchet (Scheme 5) relies on the position of the macrocycle influencing the rate of benzoylation, with acylation taking place preferentially far from the macrocycle.

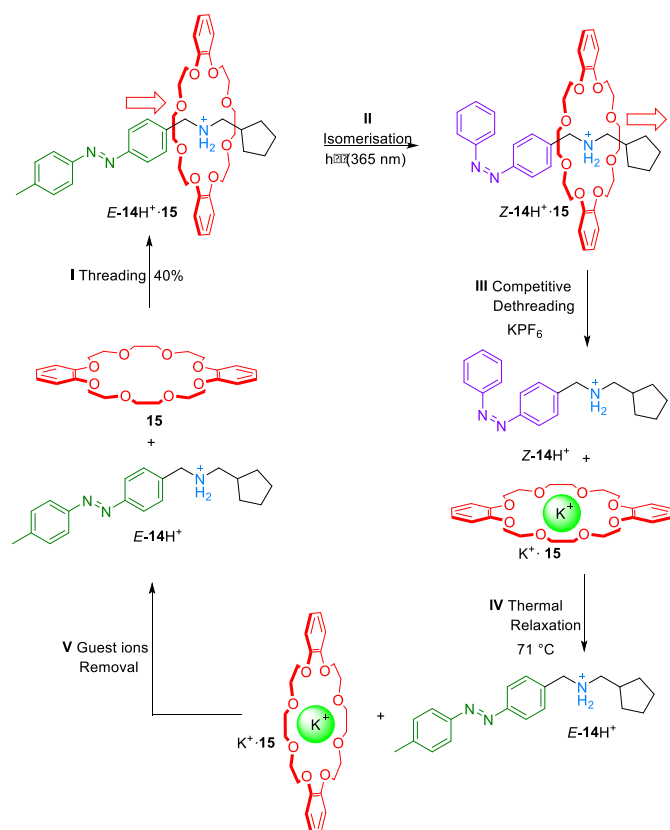


Scheme 4 Molecular information ratchet **7** and its distribution after acylation under different conditions: (a) with an achiral catalyst DMAP, (b) with chiral catalyst (*S*)-**8**, (c) with the catalyst's enantiomer, (*R*)-**8**.



Scheme 5 Molecular information ratchet **10** and its distribution after acylation under different conditions: (a) with a chiral catalyst, (*S*)-**11**, (b) with the catalyst's enantiomer, (*R*)-**11**, (c) with an achiral catalyst, (d) with a racemic mixture of the chiral catalyst.

In 2012 Credi described an energy ratchet featuring the directional threading of an asymmetric axle through a macrocycle in response to photochemical and chemical stimuli (Scheme 6).⁵⁶ The axle features a cyclopentane ring, an ammonium recognition site for a crown ether macrocycle and a photoactive azobenzene gate.⁵⁶ The strong hydrogen-bonding interaction between the macrocycle and the ammonium salt drives threading when the gate is open (*E*-isomer). The bulkiness of the cyclopentane group means that threading occurs over the other terminus. Addition of K^+ ions provides a thermodynamic driving force for dethreading (K^+ binding to the macrocycle). Closing of the gate (*Z*-isomer) ensures directional dethreading over the cyclopentane group. The same group later reported a change in the structure of the macrocycle which allowed for the spontaneous dethreading of the macrocycle without the need for a competitive guest, enabling the light-powered system to operate under continuous irradiation.⁵⁷



Scheme 6. Credi's energy ratchet pseudo-rotaxane.⁵⁶ Hydrogen bonding between the macrocycle and the ammonium group drives threading when the gate is open (*E*-isomer). Closing of the gate (*Z*-isomer) followed by competitive binding of the macrocycle allows for the directional dethreading. Red arrow indicates the direction of threading/dethreading of the macrocycle.

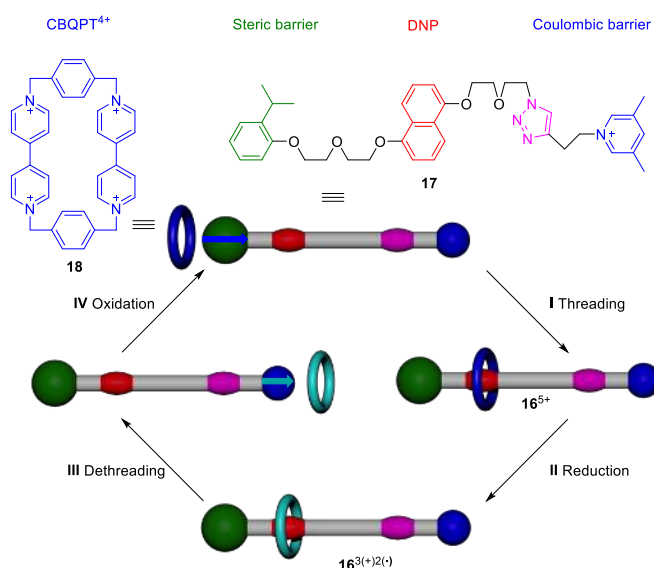


Figure 6. Stoddart's energy ratchet pseudo-rotaxane.⁵⁸ Threading of the macrocycle over the steric barrier is driven by binding between the macrocycle and the dioxynaphthalene (DNP) unit. Reduction of the macrocycle leads to the ring preferentially dethreading over the physically smaller coulombic barrier.

Similar directional translation of an axle through a macrocycle in a pseudo-rotaxane using an energy ratchet mechanism has also been recently reported by Stoddart^{58,59} (Figure 6). The pseudo-rotaxane (**16**) consists of a tetracationic cyclophane which is reduced to its radical form CBPQT^{2(•+)} with Zn dust, weakening the interaction between the ring and the dioxynaphthalene (DNP) unit. Moreover, the electrostatic repulsion between the macrocycle and the pyridinium 'coulombic barrier' is less pronounced, meaning the macrocycle dethreads over that group in preference to the bulkier 'steric barrier'. Regeneration of CBPQT⁴⁺ by exposure to air reverts the mixture to dissociated **17** and **18**.

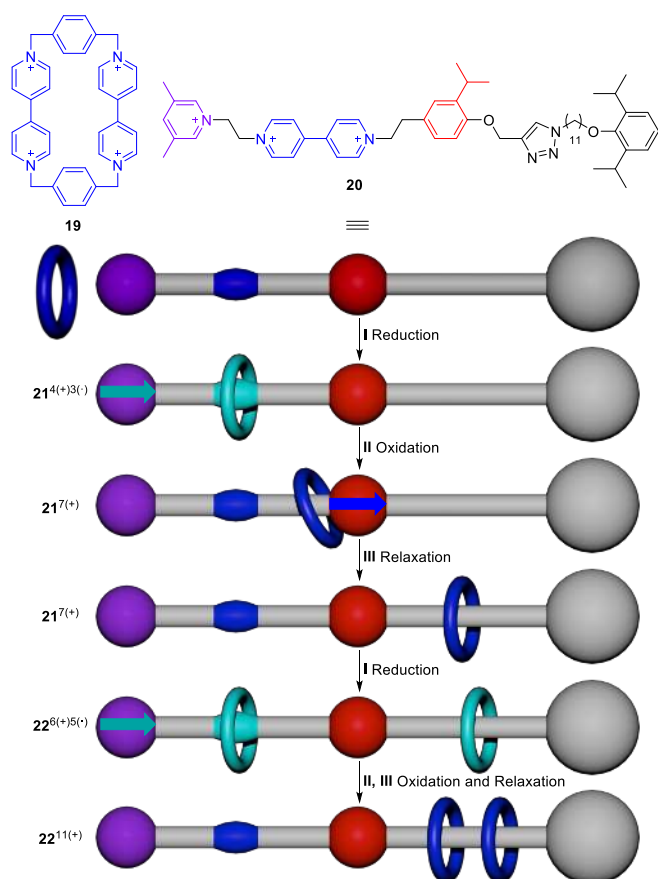


Figure 7. Stoddart's energy ratchet (pseudo)rotaxane.⁶⁰ Reduction of the macrocycle and the recognition unit drives the threading over the coulombic barrier (which is inactive under these conditions). Oxidation drives the macrocycle away from the recognition site and the active coulombic barrier, overcoming the steric barrier to reach the ring-collection domain. A second reduction, oxidation and relaxation cycle transports a second macrocycle from the solution unto the ring-collection domain, trapping the components of the [3]rotaxane in a high energy state.

A similar system has been used to thread two rings onto an axle with a single recognition site (Figure 7).⁶⁰ The addition of an oligomethylene chain, terminated by a bulky 2,6-diisopropylphenyl stopper, allows for the accumulation of two tetracationic rings on the axle after several operations. The recognition unit is altered to a redox-switchable viologen, whereas the pseudo-stoppers remain as 2-isopropylphenyl group and a positively charged 3,5-dimethylpyridinium (Figure 7). The operation cycle begins with reduction of the viologen and the CBPQT⁴⁺ ring which lessens the repulsion between the ring and the 3,5-dimethylpyridinium group while also creating an attractive force between the ring (CBPQT²⁽⁺⁾) and the viologen⁽⁺⁾. Consequently, a ring from solution slides over the pyridinium group and onto the viologen motif to form a thermodynamically stable tris-radical tricationic complex **19**^{4(+)³⁽⁺⁾. Subsequent oxidation returns the components back}

to their fully charged forms destabilising the interaction between the ring and viologen unit. Dethreading of the ring is hindered by the coulombic repulsion between the tetracationic ring, the positively charged 3,5-dimethylpyridinium pseudo-stopper and the viologen dication. Upon thermal relaxation, the ring slowly slides over the 'speed bump' and moves into the ring-collection domain.

In order to transport a second ring onto the ring-collection domain, the above process is repeated but without allowing the reverse transport of the first ring. Upon reduction, reverse transport of the first ring toward the viologen unit is inhibited by steric repulsion with the isopropylphenyl unit. In the absence of the repulsive force to propel the ring from the viologen unit (in the oxidised state **21**⁷⁽⁺⁾), the isopropylphenyl group presents a significant kinetic barrier. Instead, another ring from the bulk is threaded onto the axle. Subsequent oxidation pumps the second ring onto the collection domain. The operation of the energy ratchet transports the rings energetically uphill, as shown with earlier energy ratchets (e.g. Figure 1).

2.3 Catenane rotary motors

As discussed in Section 2.2, rotaxane architectures can be used to pump a ring distribution away from equilibrium through ratchet mechanisms. However, unless the rings dethread from a different terminus to the one where they threaded, the system will reach a steady-state in which no more work can be done. The circular way of a ratcheted ring in a catenane means that although a steady-state in the distribution of the components is reached, directional motion can continue and work continue to be done with such a molecular rotary motor (Figure 8).

Sauvage was the first to demonstrate a degree of control, albeit non-directional, over rotary movement of the components in catenanes. In a series of catenanes,^{61,62} the most sophisticated being **23** (Figure 9), the Strasbourg group were able to switch the relative orientation of the rings in catenanes using both electrochemical and photochemical stimuli. In catenane **23** each ring contains a bidentate dpp unit and tridentate terpy site.⁶² In *dpp-dpp-23*·Cu^I, the copper coordinates to the two dpp units in the usual tetrahedral arrangement. Oxidation of the metal center (by either chemical or electrochemical means) reverses the order of preference for coordination numbers (the preferred order for Cu^{II} is 6>5>4). The result is circumvolution of the rings to give the preferred hexa-coordinated species *terpy-terpy-23*·Cu^{II}. It was demonstrated that this process occurs via revolution of one ring to give an intermediate 5-coordinate species (*dpp-terpy-23*·Cu^{II}). In comparison to many related transition-metal-coordinated systems the process is relatively fast, the ligand rearrangement occurring on the timescale of tens of seconds. The process is completely reversible, via the same 5-coordinate geometry, on reduction to Cu^I (i.e. via *dpp-terpy-23*·Cu^I).⁶²

Catenane rotary motors were the first molecular machine systems to be designed to exploit Brownian ratchet mechanisms.⁴³ In [3]catenane rotary motor **24** the larger macrocycle acts as a track with four binding sites: fumaramide (A, green), tertiary fumaramide (B, red), succinamide (C, orange) and amide (D, purple), which have relative binding affinities for benzylic amide macrocycles in the order A>B>C>D (scheme 7).⁶³ Fumaramide station A is located next to a benzophenone unit allowing selective photosensitisation over the tertiary fumaramide station B. In the catenane motor's initial state the two benzylic amide macrocycles reside over the two fumaramide stations. Photosensitized isomerisation

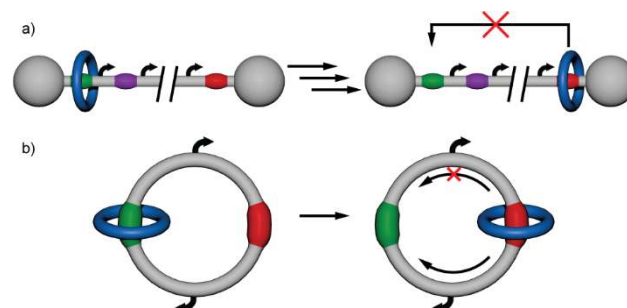
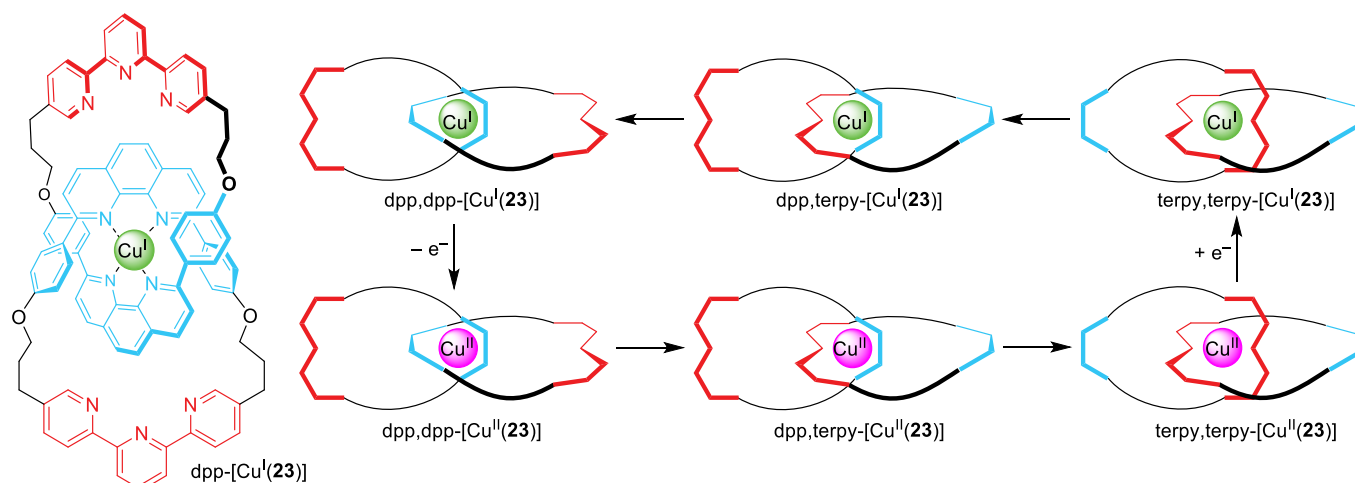


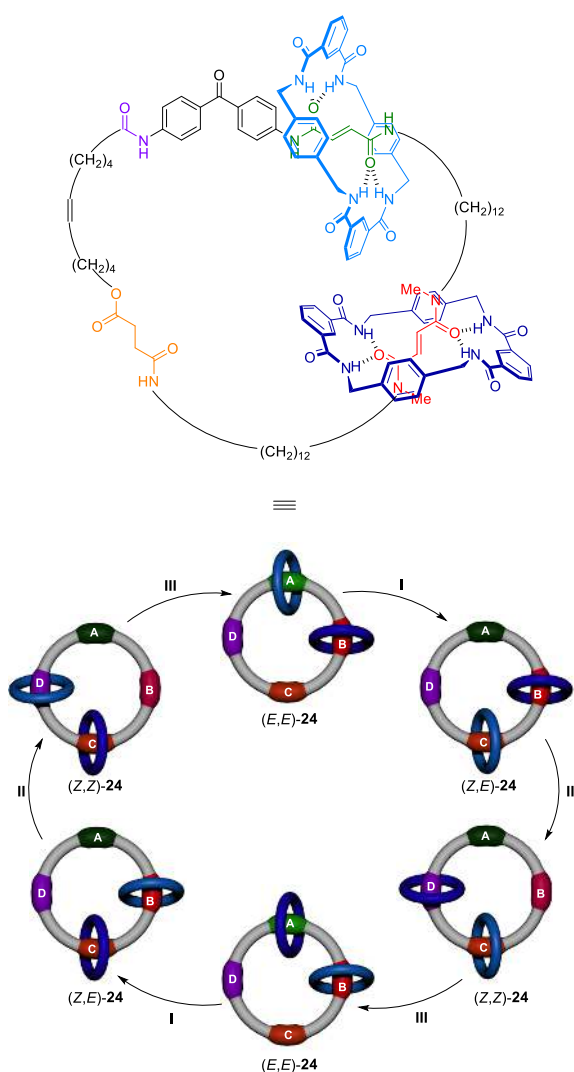
Figure 8. (a) Transport of a macrocycle in a compartmentalised rotaxane; for the machine to be reset the macrocycle has to dethread or follow a reciprocal path; (b) a compartmentalised catenane can return the macrocycle to its starting position through a different pathway.

of station A (350 nm, green → dark green) weakens hydrogen bonding interactions between the macrocycle and the station and induces macrocycle translocation to the next most favoured site, succinamide ester station C. Crucially, the presence of the second macrocycle on the tertiary fumaramide station forces this translocation to occur in an anti-clockwise fashion. Subsequent photoisomerisation of the tertiary fumaramide station (B) triggers macrocycle shuttling to binding site D. To reach its destination the macrocycle can only proceed in an anti-clockwise route. Thermal re-isomerisation restores the original binding order A>B>C>D and regenerates (*E,E-24*) but with the positions of the macrocycles swapped. This 'follow-the-leader' process in which each small ring controls the direction of circumrotation of the other, was used to directionally transport the smaller rings around the larger one.

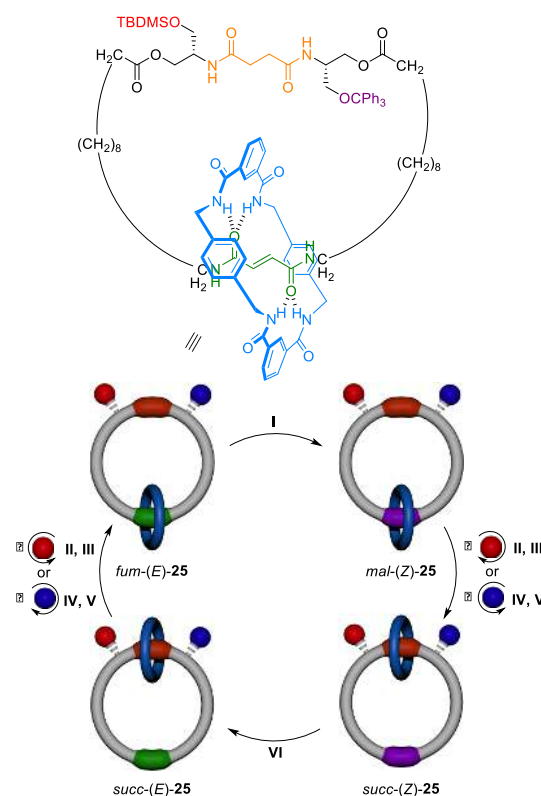
Selective rotation in either direction was achieved in [2]catenane rotary motor **25** (scheme 8) which comprises a benzylic amide macrocycle locked onto a large macrocycle bearing a fumaramide residue together with a succinamide group flanked by two orthogonally removable bulky groups: a base-labile *t*-butyl-dimethylsilyl group and an acid-labile trityl group.⁶⁴ The direction in which the benzylic amide macrocycle is transported is determined by the order in which the bulky blocking groups are removed. The first step to create a thermodynamic driving force to change the distribution of the ring between the two binding sites is photoisomerisation of *fum*-(*E*)-**25** to *mal*-(*Z*)-**25**. Next, a linking stimulus is applied: removal of one of the protecting groups (silyl for clockwise transport of the ring, trityl for anti-clockwise) results in directional displacement of the small ring to the succinamide station, the new energy minima. Reprotection unlinks the compartments and traps the macrocycle on the succinamide group. Isomerisation of the maleamide station back to fumaramide restores the original thermodynamic preference



for the macrocycle to shuttle back to the fumaramide station. Removal of the second blocking group results in full 360° rotation of the small macrocycle around the larger one.



Scheme 7. Directional circumrotation in sequentially operated [3]catenane rotary motor **24**: (I) $h\nu$ (350 nm); (II) $h\nu$ (254 nm); (III) Δ , or Δ with catalytic ethylenediamine, or catalytic Br, $h\nu$ (400–670 nm).



Scheme 8. Reversible 360° rotation in sequentially operated [2]catenane rotary motor **25**: (I) $E \rightarrow Z$ $h\nu$ (254 nm); (II) TBAF; (III) TBDMSOTf; (IV) $\text{Me}_2\text{S} \cdot \text{BCl}_3$; (V) TrOTf; (VI) $Z \rightarrow E$ piperidine.

The catenane motors shown in schemes 7 and 8 require sequences of chemical transformation for 360° directional rotation to occur. Recently, Leigh and colleagues described a chemically-driven molecular motor that can operate autonomously, that is directional rotation continues so long as unreacted fuel remains (Figure 10).⁶⁵ This two-compartment [2]catenane rotary motor operates through an information ratchet mechanism. Directional transport of the small macrocycle around the larger one is promoted by an acylation reaction using a sterically-demanding pyridine-based catalyst. Catenane **26** features fumaramide groups (shown in green) on the larger ring (the 'track') which serve as binding sites for a benzylic amide macrocycle (blue). Bulky 9-fluorenylmethoxycarbonyl groups (red) sterically block passage of the small blue ring and trap it in one compartment or the other (the right- or left-hand side of the track as shown). Cleavage of one of the bulky groups through a chemical reaction (loss of orange ball) allows the small ring to shuttle back and forth between the two fumaramide sites on the track via Brownian motion along the unblocked pathway. Attachment of another bulky group (addition of red ball)

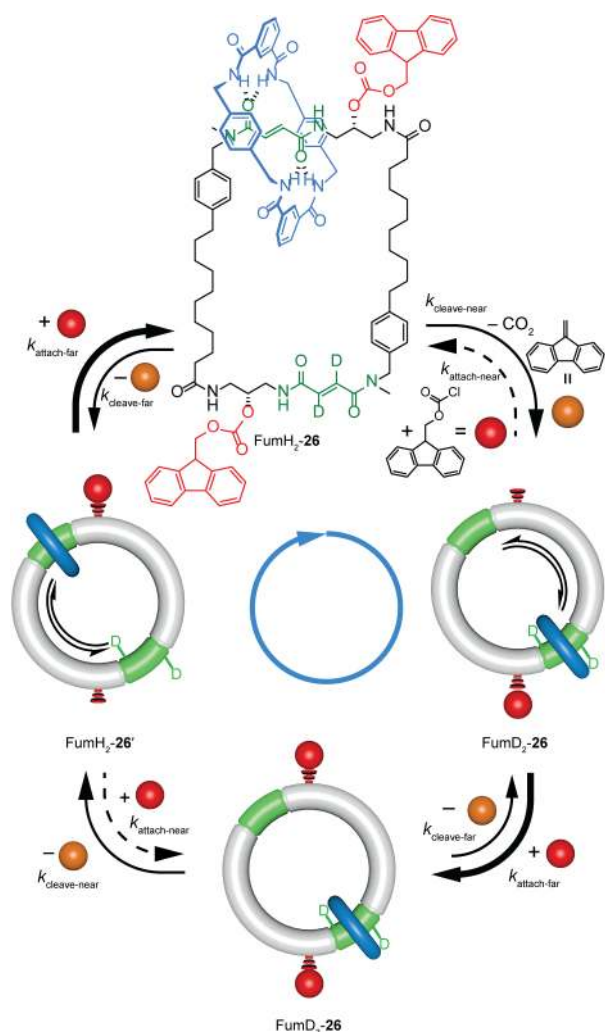


Figure 10. An autonomous chemically-fuelled [2]catenane rotary motor. Bold arrows indicate the major pathway of reaction, dashed arrows indicate the minor pathway and thin arrows indicate pathways that occur at similar rates. The blue arrow indicates the direction of net transport of the benzylic amide macrocycle when $k_{\text{attach-far}} > k_{\text{attach-near}}$ and $k_{\text{cleave-far}} = k_{\text{cleave-near}}$.⁶⁵ Reproduced from Ref. 65 with permission from Macmillan Publishers Ltd, copyright 2016.

through another chemical reaction (under the same conditions) locks in any change of location of the small ring (that is, if the ring has changed compartment it is prevented from returning to the original one). Key to the design is that the rate of reaction of this fuel with reactive sites on the cyclic track is faster when the macrocycle is far from the reactive site than when it is near to it. Since the kinetics for blocking group attachment are faster when the small ring is far from the reactive site ($k_{\text{attach-far}} > k_{\text{attach-near}}$), but the cleavage reaction occurs at a rate independent of the small ring position ($k_{\text{cleave-far}} = k_{\text{cleave-near}}$), then the small ring directionally rotates around the larger one. Under reaction conditions where both attachment and cleavage of the blocking groups occur through different processes, and the cleavage reaction occurs at a rate independent of macrocycle location, net directional rotation of the molecular motor continues for as long as unreacted fuel remains. Just as motor proteins catalyse the hydrolysis of ATP, catenane **26** acts as a catalyst for the conversion of Fmoc-Cl NEt_3 into dibenzofulvene, CO_2 and Et_3NHCl waste products, and it is the energy released by these reactions which drives

the directional displacement of the small macrocycle around the larger one. By linking the position of the macrocycle to more efficient catalytic consumption of the fuel, faster and more efficient small-molecule motors should be possible.

3. Rotary Motion in Non-Interlocked Structures

3.1 Rotation around a single bond

In this section, we will discuss three types of molecular motors which exhibit rotary motion around a covalent bond as the axle. Chemically fueled motors which rotate around a single bond, and light fueled motors which rotate around a double bond. Within the second class, a distinction is made between symmetrical designs (1st generation motors) and asymmetrical designs (2nd generation motors and imine based motors) (Figure 11).

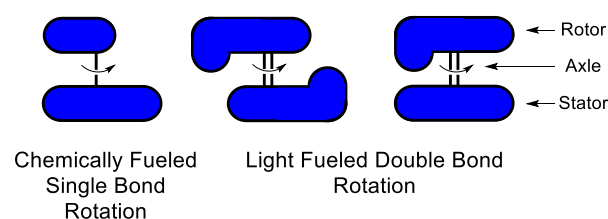


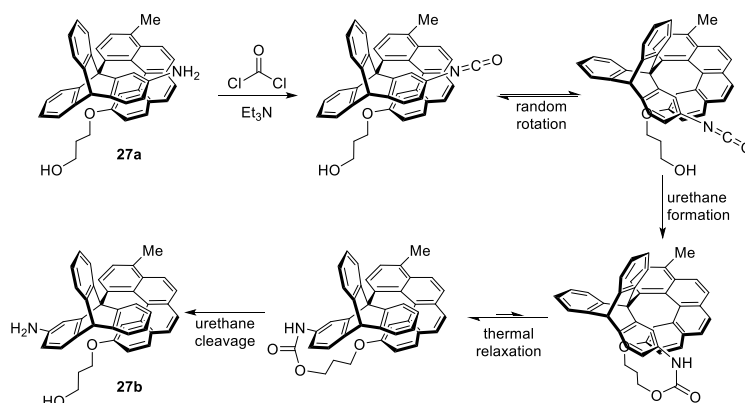
Figure 11. Classes of rotary molecular motors discussed in this section.

Rotary motion is inherent in single bonds, but directional control of this motion is a challenging target. Basic requirements for a rotary motor based on rotation around an axle are: the rotation should be powered by fuel, control of directionality is needed and the process should be repetitive to enable continuous motion. Early investigations in this area aimed at the development of molecular ratchets, but failed to meet all of the criteria. These molecules contain a gear which is able to rotate freely in one direction while a pawl attempts to prevent rotation in the other direction.

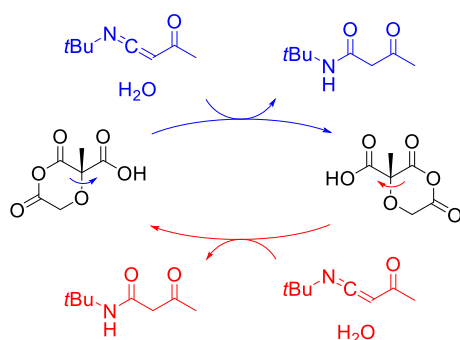
The group of Kelly developed several ratchet-type molecules,^{12,66,67} leading up to their report of a chemically driven rotor, capable of performing 120° unidirectional rotation around a single bond in two chemical steps.^{68,69} This device, much like their previous designs, consists of a triptycene 'wheel' and a helicene 'brake', connected by a single bond. The brake raises the barrier of rotation around the aryl-aryl bond to 25 kcal/mol, thereby severely hindering rotation of the wheel. Although the helicity of the system induces a desymmetrization of the energy profile of the rotation around the single bond, the rate of rotation is equal in both directions as predicted by the Second Law of Thermodynamics.⁷⁰ The authors manage to force unidirectionality on the rotation by the modification of the structure with a primary alcohol tethered to the helicene, and an amine group on one of the wheels of the triptycene. At room temperature, the compound exists as a mixture of three atropisomers. Addition of phosgene to atropisomer **27a** generates an isocyanate on the triptycene moiety (Scheme 9).

Thermal clockwise rotation of the wheel brings the isocyanate sufficiently close to the primary alcohol for urethane formation, generating a sterically constrained conformer. Thermal energy drives the unidirectional rotation, overcoming the barrier of rotation around the single bond. Subsequent cleavage of the urethane leads to formation of atropisomer **27b**. Although the unidirectional motion is limited to a single, non-repeatable 120° rotation and phosgene is an undesirable choice of fuel, this work does however constitute a milestone in the search for continuous directed molecular motion. Follow-up publications explored the possibility of continuous rotation, although these efforts have not yet been successful.^{71,72}

In 2003, Mock and Ochwat presented what is perhaps the most basic approach towards a molecular motor design reported thus far (Scheme 10).⁷³ The tricarboxylate motor oscillates between two anhydride forms and is fueled by an acylketenimine. The process is continuous as long as fuel is present. Although one cycle causes a 180° unidirectional rotation, the following cycle causes the reverse rotation and no net directional rotation is generated. A very different approach towards directional motion is the system developed by Haberhauer, which utilizes metal complexation and decomplexation as vital steps in the rotary cycle.⁷⁴ This motor consists of two bipyridine moieties, linked by a cyclic peptide and an ethane bridge. One of these bipyridines has an azobenzene substituent. A full 360° rotation proceeds in four steps of alternating azobenzene photoisomerisation and bipyridine complexation/decomplexation. Unidirectionality was not proven experimentally but through DFT calculations.



Scheme 9: Phosgene induced 120° unidirectional rotation around the triptycene-helicene single bond. (a) Fuel addition, (b) Thermally driven single bond rotation, (c) Linking, (d) Unidirectional rotation leading to strain release, (e) Release. Reproduced with permission from ref 68, Macmillan Publishers Ltd, copyright 1999.

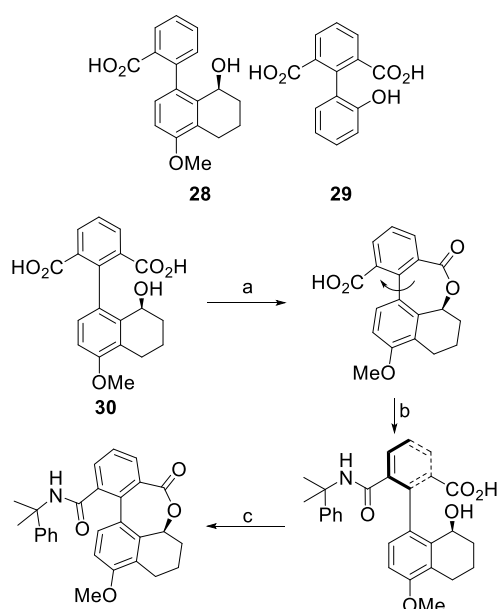


Scheme 10: Acylketenimine fueled oscillation of anhydride motor.

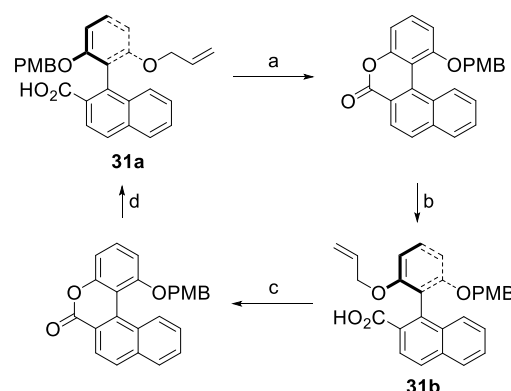
2 Biaryl based rotary motors

Certain biaryls have a sterically hindered rotation around the central single bond and are therefore a practical starting point for the design of directional rotors. Several attempts towards directional rotors have been undertaken based on diastereoselective nucleophilic ring-opening of biaryl lactones.⁷⁸ The initial design **28** (Scheme 11), based on studies by Bringmann,⁷⁵ featured a biaryl functionalized with an alcohol and a carboxylic acid functionality in the ortho positions on each side of the aryl-aryl bond.⁷⁶ Lactonization and subsequent ring-opening were successful, but due to the fast equilibrium of the atropisomers the directionality of this system could not be determined. Subsequently, Branchaud and co-workers developed a tri-ortho substituted biaryl **29** (Scheme 11), functionalized with two carboxylic acid moieties on one aryl group and an alcohol substituent on the other aryl group.⁷⁷ This modification raised the barrier of rotation around the single bond sufficiently compared to their previous design,

and the efficiency of unidirectional rotation was determined to be 20% or 50%, depending on the choice of chiral auxiliary. The unidirectionality could be improved by introducing a slight change in the design and using a bulkier nucleophile (**30**, Scheme 11).⁷⁸ Using this combination of biaryl and nucleophile, diastereoselective ring-opening followed by chemoselective re-lactonization causes a 180° rotation with a very high diastereoselectivity (>99% by ¹H NMR analysis) and 72% yield. The authors note that if the resulting amide could be cleaved selectively, the system should be capable of a six step 360° rotation. However, no such conditions have been reported thus far. Feringa and co-workers demonstrated a sequentially operated chemically-driven rotary motor, when they reported a tri-ortho substituted biaryl, **31**, capable of unidirectional rotation (Scheme 12).⁷⁹ However, they achieved a higher unidirectionality and 360° rotation by making a few modifications. Starting from atropisomer **31a** the allyl protecting group can be selectively removed, after which the newly deprotected phenol can be lactonized with the carboxylic acid functionality on the lower half. An asymmetric reductive ring-opening using an auxiliary chiral reducing agent generates a phenol and a primary alcohol. After selective re-protection of the phenol with an allyl protecting group, the alcohol can be oxidized to the carboxylic acid and the atropisomer **31b** is formed. In analogous fashion, the *para*-methoxy benzyl (PMB) protecting group can be removed selectively, after which the sequence of lactonization, asymmetric ring opening, reinstallation of the protecting group and oxidation can be repeated and atropisomer **31a** is regenerated. Because the ring openings both proceed with excellent enantioselectivities, both halves of the cycle are > 90% unidirectional. Crucially, racemization of the

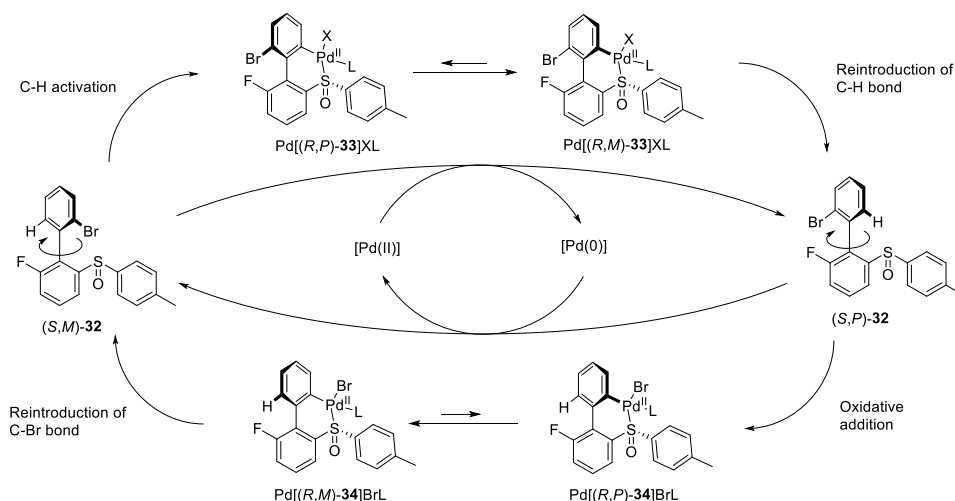


atropisomers does not occur at room temperature since the barrier of rotation around the aryl-aryl bond is too high. Additionally, due to the choice of protecting groups, the two deprotection steps completely orthogonal. Furthermore, this system has the capacity to reverse its rotary direction by changing the sequence of chemical steps. Although ten steps are required and the overall yield for a cycle is 21%, this reversible rotary motor is the first system reported to undergo a chemically driven 360° rotation around a C-C single bond. A major disadvantage of all the systems discussed in this section is the need for sequential addition of fuels. For the generation of motion, a synthetic molecular motor should be able to operate continuously under a specific set of reaction conditions. Continuous photochemically driven rotary motion has been achieved (see Section 3.4),⁸⁰ but designing chemically fueled analogues remains challenging. Recently, Feringa and co-workers made significant steps towards such a system with a unidirectional biaryl, fueled by a palladium redox cycle.⁸¹ Scheme 13 shows the 360° rotation cycle. The motor contains a two-fold chirality: a fixed chirality at the sulfur atom which governs the direction of rotation, and an axial chirality around the biaryl single bond. No racemization occurs since in atropisomers (*S,M*)-**32** and (*S,P*)-**32** the barrier of single bond rotation is too high to occur spontaneously at room temperature. Starting from atropisomer (*S,M*)-**32**, palladacycle



Scheme 12: Rotational cycle of unidirectional biaryl motor reported by Feringa and co-workers. (a) Allyl deprotection and lactonization, (b) asymmetric lactone reduction, reinstallation of the allyl protecting group and oxidation to reform the carboxylic acid, (c) *para*-methoxy benzyl deprotection and lactonisation, (d) asymmetric lactone reduction, reinstallation of the PMB protecting group and oxidation to reform the carboxylic acid.

Pd[(*R,P*)-**33**]XL can be formed through a C-H activation event. Because a Pd(II) source is used, and the sulfoxide acts as a directing group, this process is selective for the *ortho* C-H bond on the upper aryl ring. In this palladocycle the barrier of rotation around the biaryl axis is greatly reduced. DFT calculations show that *M* helicity around the biaryl axis is favoured, leading to a net clockwise rotation. Therefore, when the C-H bond is subsequently reintroduced, the reductive elimination proceeds mainly from Pd[(*R,M*)-**33**]XL and (*S,P*)-**32** is obtained in excellent (>98%) stereoselectivity and a 45% overall yield. The unidirectional transformation of (*S,P*)-**32** in (*S,M*)-**32** could be achieved in analogous fashion. By addition of a Pd(0) source, C-Br activation could be achieved and palladocycle Pd[(*R,P*)-**34**]BrL was formed. *M* helicity is favoured in this palladocycle too, and the subsequent bromination occurred mainly on Pd[(*R,M*)-**34**]BrL. (*S,P*)-**32** was obtained in 92% selectivity and 42% overall yield. The two 180° unidirectional rotations that are thus achieved, are completely orthogonal to each other and connected through a redox cycle: one rotation leads to a conversion of a palladium(II) source into a palladium(0) source and the other converts a palladium(0) source into a palladium(II) source. In fact, after unidirectional transformation of (*S,M*)-**32** to (*S,P*)-**32**, the *in situ* formed palladium(0) could be used to catalyze the transformation (*S,P*)-**32** to (*S,M*)-**32**, thereby completing a 360° unidirectional rotation. By careful selection of reaction conditions, and provided chemical fuel is present, this system may be used to generate continuous rotational motion without the need of sequential fuel addition or purification.



Scheme 13: Unidirectional rotation around the biaryl single bond, driven by a palladium redox cycle.

3.3 Electrically-driven motors

With the exception of the partially photochemically driven motor presented by Haberhauer,⁷⁴ all of the above examples of directional single bond based rotary motors are fueled by chemical reactions. Sykes and co-workers studied the directionality of electrically driven motors.⁸² Surface-bound butyl methyl sulfide rotors (Figure 12) exist as two enantiomers, since either one of the sulfur lone pairs may bond with the surface. Thermally induced rotation around the sulfur-surface bond was found to be random. Excitation with an STM tip led to a 5% directionality for one enantiomer, and no preference of direction but an increase in rotation speed for the other enantiomer. This behaviour was attributed to the intrinsic chirality of the STM tip.⁸³ Control experiments with an achiral STM tip did not cause a measurable difference in rate or direction between both enantiomers.

3.4 Rotation around double bonds

In 1999 Feringa et al reported on the first light-driven molecular motor capable of performing repetitive unidirectional 360° rotation.⁸⁰ The motor was based on an overcrowded alkene featuring a double bond connecting two identical halves or rotor parts. Due to the severe steric interaction present in the system, the double bond is forced out of planarity, giving a helical shape to the molecule, which proved to be key in the functioning of these systems. For the (R,R) enantiomer of **35**, four different isomers exist, which can

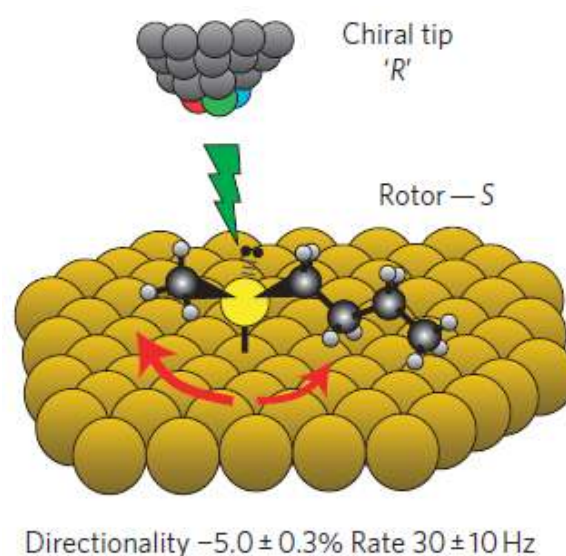
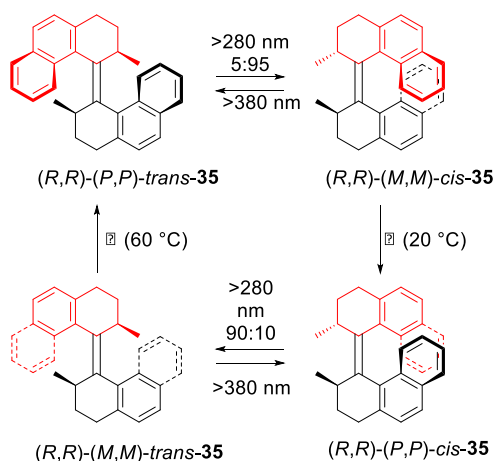


Figure 12: Representation of surface-bound butyl methyl sulfide rotor. The combination of a chiral tip with *R* chirality and a rotor with *S* chirality leads to 5% directionality of rotation around the sulfur-surface bond. Reproduced with permission from ref 82, Macmillan Publishers Ltd, copyright 2011.

be interconverted in four discrete steps with light and heat in such a way that unidirectional rotation around the carbon-carbon double bond (the rotation axle) is achieved (Scheme 14). Starting from $(P,P)\text{-trans-}35$, irradiation with UV light induces a photochemical *trans-cis* isomerization of the double bond leading to the formation of



Scheme 14: Mechanism for unidirectional 360° rotation for the first-generation light-driven molecular motor.

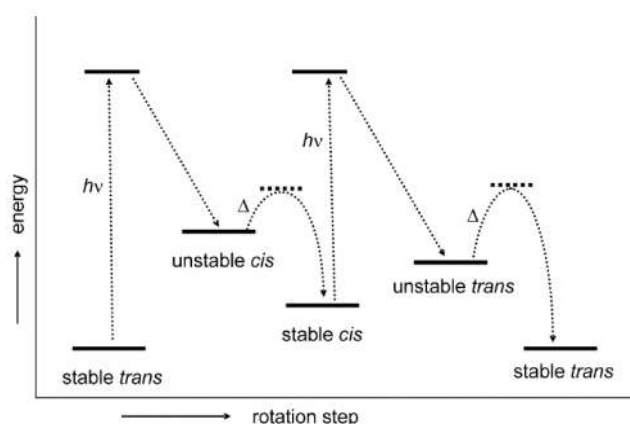
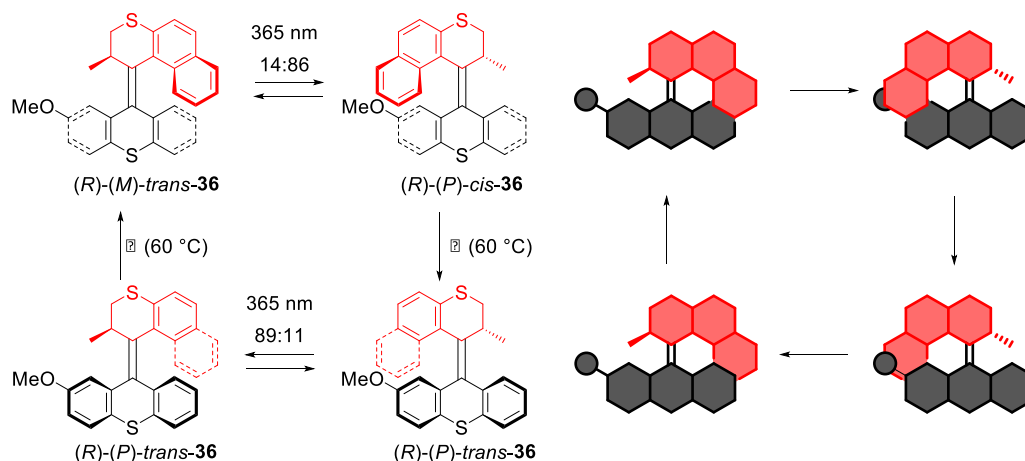


Figure 13: General energy profile for the 360° unidirectional rotation.

(*M,M*)-*cis*-**35**. During this event, the helicity of each half inverts, while the methyl groups change from a pseudoaxial orientation to a pseudoequatorial orientation. The newly formed (*M,M*)-*cis*-**35** is higher in energy, due to increased strain caused by equatorial position of the methyl groups. These methyl groups can again adopt their energetically favoured position by a thermal relaxation process of the molecule, in which one half flips over the other half, affording (*P,P*)-*cis*-**35**. In addition to the reorientation of the methyl groups, the helicity of the molecule is inverted once again. This relaxation is called a thermal helix inversion (THI) and, in principle, is an equilibrium reaction but since the energy difference between the stable and unstable form is large, this step can be considered irreversible, thereby biasing the direction of rotation. A second photochemical isomerization gives rise to the isomerization of (*P,P*)-*cis*-**35** to give the unstable (*M,M*)-*trans*-**35**. (*M,M*)-*trans*-**35** undergoes a THI to return to (*P,P*)-*trans*-**35**, the starting point of this 360° cycle. During these four isomerization steps, one half has completed a 360° rotation relative to the other half around the double bond. The energy profile of the ground state and excited state of this light-driven process are schematically depicted in an energy diagram (Figure 13). This mechanism is from a

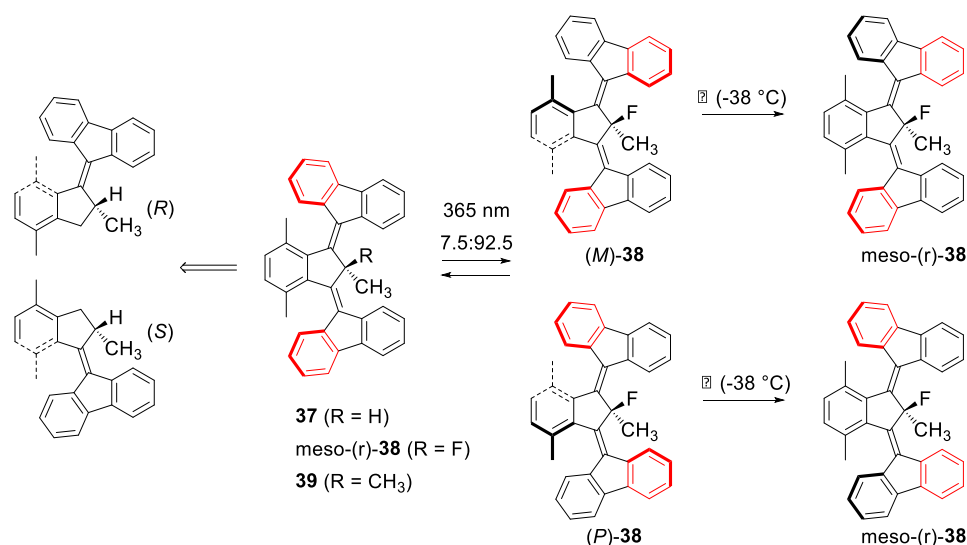
stereochemical point of view a beautiful interplay between the dynamic helical chirality present in the molecule and the fixed point chirality of the stereogenic centres. The helicity inverts in every isomerization step, while the configuration of the stereogenic centre dictates the direction of rotation. The energetically uphill *E-Z* isomerization drives the system out of equilibrium, while the subsequent energetically downhill THI ensures that the motor returns in its stable form, from which it can be excited again, leading to a repetitive process as long as light is supplied as fuel for this rotary motion. This system has the characteristics of a power-stroke motor. A disadvantage of these first generation molecular motors is that the activation barrier for the thermal isomerization steps are not similar. One half of the 360° rotation is therefore considerably faster than the other, which results in an irregular rotation. This issue was addressed by a second design of the overcrowded alkene molecular motor.⁸⁴ One of the halves connected to the double bond was replaced by a symmetrical (apart from the methoxy substituent) lower half to afford **36** (Scheme 15). For second generation overcrowded alkene molecular motors, the upper half is usually referred to as the rotor, while the lower half is called stator, although in reality it concerns a relative rotation of one half to the other, rather than one part moving and one part standing still. A major advantage of 2nd generation motors is the ready functionalization of upper (rotor) and lower (stator) parts, for instance for surface anchoring. The structural modification resulted in very similar barriers for both THIs and therefore a more uniform rotation. Although the 2nd generation overcrowded alkene molecular motors are structurally quite different from 1st generation overcrowded alkene rotors, the same mechanistic steps account for the functioning as a molecular motor. A key finding in the development of the 2nd generation overcrowded alkene molecular motor was that one stereogenic centre proved to be sufficient in achieving unidirectionality. The reduction in chiral information led to the question how much chirality is actually needed to achieve unidirectionality in these systems. To this end the so called 3rd generation overcrowded alkene molecular motor was developed.⁸⁵ The design of this motor was conceived by merging two 2nd generation overcrowded alkene motors together in such a way that the stereocenter becomes a pseudo asymmetric centre thereby making the whole molecule achiral.^{86,87} The design of the 3rd generation overcrowded alkene motor and its mode of rotation are depicted in Scheme 16. As is the case for the 1st and 2nd generation overcrowded alkene molecular motors, the (pseudo) asymmetric centre has groups of two distinct different size (CH_3 and H/F) attached to it. The thermodynamically favoured isomer is the isomer where the bigger group methyl adopts a (pseudo) axial position, while the smaller H or F atom is forced in the more sterically hindered (pseudo) equatorial position. In the study published in 2014, the isomer **37** with R=H was synthetically inaccessible and thus the variant with the fluorine substituent was synthesized (**38**). It was found that for the stable isomer, the fluorine adopts the pseudo equatorial position where it is sandwiched between



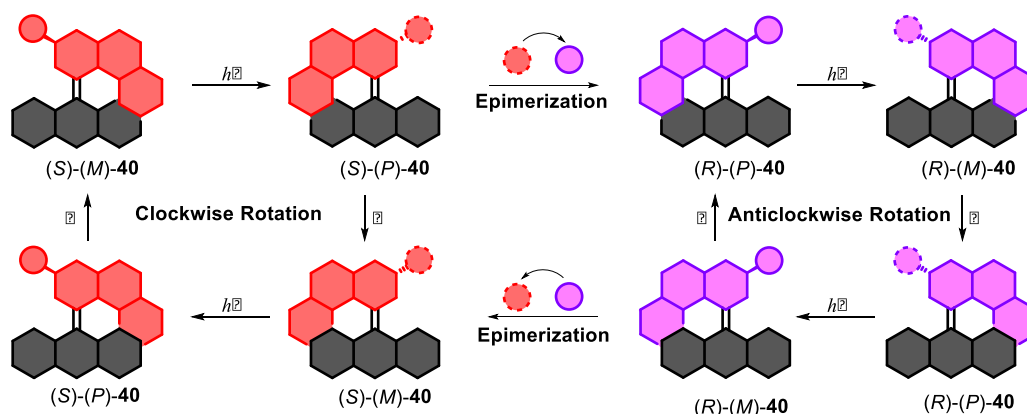
Scheme 15: (left) Mechanism for unidirectional 360° rotation for second-generation light-driven molecular motor **36**. (right) Schematic representation of this process.

the two fluorene lower halves. Starting from meso-(*r*)-**38**, irradiation with UV light (365 nm) leads to the isomerization of either one of the double bonds, giving a PSS mixture of 7.5 : 92.5 = (*r*)-**38** : (*M*)-**38** + (*P*)-**38**. The isomerization of both double bonds to give meso-(*s*)-**38** was not observed, which was attributed to the asymmetric excited state surface of (*P*)-**38** and (*M*)-**38**. The photogenerated enantiomeric pair thermally relaxes via a THI ($\Delta^\ddagger G^\circ = 75.3 \pm 0.3 \text{ kJ mol}^{-1}$) to return to the starting meso-(*r*)-**38**. The possibility of a thermal relaxation via a backward thermal *E-Z* isomerization (TEZI), could not be ruled out in this system, since the product of the two reactions are the same. For this reason a second design was conceived in which the rotor parts were desymmetrized by the introduction of the methoxy group. It was found that **38** functions as a unidirectional rotor and no thermal back TEZI occurs. From the studies on the thermal behaviour of many other molecular motors, it is evident that in general the TEZI becomes a competing pathway, only when the $\Delta^\ddagger G^\circ$ for THI is sufficiently high ($>110 \text{ kJ mol}^{-1}$).⁸⁸ In this sequence of light and heat induced isomerization steps for **38**, one rotor part performed a 180° clockwise rotation, while the other rotor part performed a 180° anticlockwise rotation, relative to the middle stator part (Scheme 16). For an external observer, both rotor parts thus move in the same forward direction, similarly to wheels on an axle. From the point of a single molecule, the absorption of a photon can lead to either 180° anticlockwise rotation of the upper rotor or a 180° clockwise rotation of the lower rotor in equal probability. For a system where $R=\text{CH}_3$ (**39**), no directionality would be expected in the rotational behaviour of the rotor parts. A pseudo-asymmetric centre is therefore, to date, the minimal "chiral requirement" for dictating the directionality of rotation in overcrowded alkenes.

As well as addressing the issue of required stereochemistry for directionality, this study brought forth overcrowded alkene based motors with interesting rotational behaviour. The observed motion for these systems could potentially be harnessed for directional movement on e.g. a surface, similarly as has been reported for the nanocar (see Section 4.2). The configuration of the stereocentre controls the direction of rotation around the double bond and this aspect was used in the development of a motor that can be switched between "forward" and "reverse" rotation by a chemical stimulus.⁸⁹ A 2nd generation overcrowded alkene molecular motor was designed with an acidic proton at its stereocentre, allowing for epimerization by the action of a base (Scheme 17). Notice that in this system the stereocentre was replaced from the α to the β position, as deprotonation and subsequent reprotonation at the allylic position would most likely lead to a double bond shift of the overcrowded alkene. It is known that a stereocentre at the β position can also bias the direction of rotation, but to a lesser degree, rendering the rotation of β substituted motors not fully unidirectional.⁹⁰ Starting from the isomer (*S*)-(*M*)-**40**, photoisomerization leads to the formation of the less stable isomer (*S*)-(*P*)-**40**, which after heating to 80 °C thermally relaxes to (*S*)-(*M*)-**40**. A second cycle of an irradiation and subsequent heating step would result in a 360° clockwise rotation. At room temperature the THI is slow; (*S*)-(*P*)-**40** has a half-life of 22 d. The unstable isomer (*S*)-(*P*)-**39** could be epimerized in this timeframe into the thermodynamically favoured diastereoisomer (*R*)-(*P*)-**40** in a ratio of 91:9 by the action of 1 equivalent of *t*-pentylONa in *t*-pentanol over the course of 15 h. The newly formed isomer (*R*)-(*P*)-**40** will, under the influence of light and heat rotate in the opposite direction (i.e. anticlockwise) compared to the



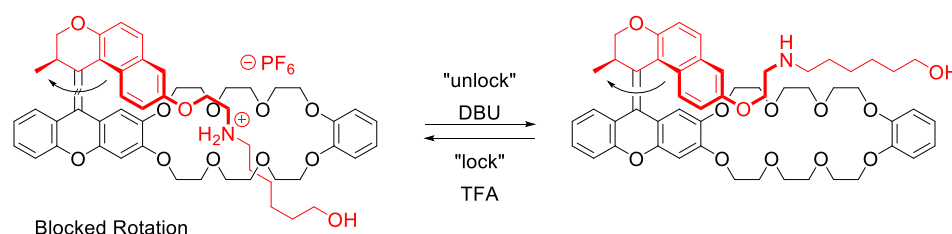
Scheme 16: Rotational behaviour of molecular motor with a pseudo-asymmetric centre.



Scheme 17: Base catalysed epimerization leading to reversal of the direction of rotation.

starting isomer. This work shows that precise control of stereochemical elements is crucial in achieving higher degrees of complexity of motion generated by molecular machines. In addition to controlling the direction of rotation by a chemical stimulus, the photochemical step and therefore the whole rotation can also be inhibited by a chemical trigger.⁹¹ The system for which this behaviour has been described consisted of a 2nd generation overcrowded alkene molecular motor functionalized with a dialkyl ammonium group on the upper half and a dibenzo[24]crown-8-ether attached to the lower half (Scheme 18). It was found by ¹H-NMR spectroscopy that in CD₂Cl₂ the ammonium group is bound non-covalently to the crown ether. In this self-complexed state the photochemical *cis-trans* isomerisation is efficiently quenched, resulting in no rotation upon irradiation. Addition of the base DBU leads to deprotonation of the ammonium group, which resulted in the dethreading of the pseudorotaxane system. In this unlocked

state, irradiation leads to photoisomerization of the double bond and the subsequent THI leads to unidirectional rotation. The rotation can again be stopped by threading the dialkylammonium group into the crown ether by the action of trifluoroacetic acid (TFA). Numerous studies have been conducted on ways of increasing the rotational speed of 1st and 2nd generation overcrowded alkene molecular motors by small structural modifications (Figure 14). Since the photochemical isomerization is substantially faster (picosecond timescale) than the thermal isomerization step,^{92,112} these studies focused on reducing the barrier for the THI. It was found that, increasing the steric bulk at the α position, causes a large acceleration.⁹³ This finding can be rationalized by the fact that the bulkier substituents in the α position destabilize the metastable state to a greater extent than the TS.



Scheme 18: Reversible locking/unlocking the rotation by chemical means.

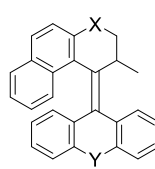
|  | X | Y | $t_{1/2}$ |
|---|-----------------|----------------------------------|-----------|
| | S | S | 215 h |
| | S | O | 26.3 h |
| | S | C(CH ₃) ₂ | 233 h |
| | CH ₂ | S | 0.67 h |
| | CH ₂ | C(CH ₃) ₂ | 2.01 h |

Figure 14: Various structural modifications in 2nd generation molecular motors.

Modifications that focus on reducing steric hindrance between the rotor part and stator part in the fjord region, also result in the acceleration of these molecular rotors. For 2nd generation overcrowded alkene molecular motors with the general structure depicted in Figure 14, it was found that the nature of the bridging atoms X and Y have a considerable impact on the rotational speed of these structures. The subtle conformational changes these modifications induce, amount to a difference in the speed of the motors up to a factor of almost 350. It was found that the contraction of the ring fused to the double bond had an even greater impact on the barrier for the THI (Figure 15). Contracting the six membered ring upper half (see compound **41**) to a five membered ring (see compound **42**) resulted in a dramatic decrease in steric hindrance in the TS which accounts for a 2×10^8 fold acceleration of the rotational speed.⁹⁴ Further reduction of the steric hindrance in the TS by replacing the naphthalene with a *p*-xyllyl (see compound **43**) or benzothiophene (see compound **44**) accelerates the motor with a factor of 12 and 2.7×10^3 , respectively.^{95,96} Although it is not always *a priori* clear whether a particular structural modification increases or decreases the activation energy of the THI,⁹⁷ DFT calculations can accurately predict the Gibbs free energy of activation for this step and is therefore a valuable tool in the design of rotary motors.⁹⁸ The continuous efforts in increasing the rotational frequency of the systems culminated in the development of motors which can operate in the MHz regime.⁹⁹ One of the fastest motors up to date, combines a thioxanthene lower half and a cyclopentane naphthalene upper half (**45**). The extremely low barrier ($\Delta^\ddagger G^\circ = 33.5 \text{ kJ mol}^{-1}$) for the THI causes this motor to rotate at this exceptional speed. Computational research even suggests that by substituting the stereogenic

methyl group with a methoxy moiety, these particular systems would in principle function way beyond the MHz regime into the GHz regime.¹⁰⁰ In 2016 a different strategy was followed for the tuning of the rotational speed.¹⁰¹ Rather than the synthesis of different variants, this approach relied on a non-covalent post synthetic modification to fine-tune the speed of the motor (Figure 16). The studied system consisted of a 4,5-diazafluorenyl lower half and naphthalene upper half (see compound **46**). The binding of different metals to the bidentate lower half led to delicate conformational changes, most notably the contraction of the diazafluorenyl half. The decrease in steric hindrance in the fjord region resulted in an increase in rotational speed. The magnitude of this increase was dependent on the choice of the transition metal complex. While the parent motor has a $\Delta^\ddagger G^\circ$ of 83.5 kJ mol^{-1} for the THI, binding of ZnCl_2 , led to a $\Delta^\ddagger G^\circ$ of 81.5 kJ mol^{-1} . Complexation of PdCl_2 and PtCl_2 resulted in a decrease in $\Delta^\ddagger G^\circ$ to 78.2 and 75.1 kJ mol^{-1} , respectively. The changes in $\Delta^\ddagger G^\circ$ reflect a more than factor 30 increase in rotational frequency and is thus a powerful method to fine tune the speed with great accuracy in a reversible and dynamic way. This work shows that by emulating Nature, and the way it regulates processes at the molecular level, e.g. allosteric regulation, fascinating design principles can come to light which can be used in the design of molecular machines. In addition these systems have the benefit of shifting the wavelength of irradiation towards the visible. Tuning of the rotational speed by electronic effects was found to be more difficult.¹⁰² The placement of either electron donating or withdrawing groups did not affect the barrier for the THI significantly. The introduction of a donor acceptor system along the double bond decreased the barrier for THI significantly, but also accelerated the thermal back reaction, rendering this type of molecular motor not fully directional.¹⁰³ Computational studies performed by Durbeej *et al.*¹⁰⁴ (*vide infra*) indicate that the introduction of electron donating groups in the 3 and 6 position of motor **43** would lead to a significant reduction of the $\Delta^\ddagger G^\circ$ for THI.¹⁰⁴ Tuning the rotational speed by electronic effects would be a nice complementary approach to tuning via

ARTICLE

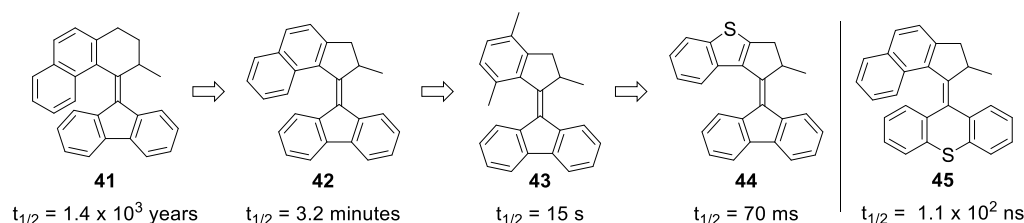


Figure 15: Incremental increase of rotational speed by structural modifications. The $t_{1/2}$ refers to the half-life of the photogenerated metastable isomer at 25 °C and is inversely related to the rotational speed

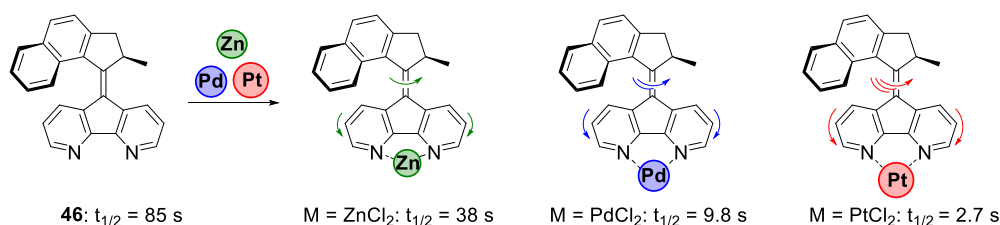


Figure 16: Molecular motor with tuneable rotational speed. The $t_{1/2}$ refers to the half-life of the photogenerated metastable isomer at 25 °C.

steric effects, but has not yet been investigated thoroughly. The application of light driven motors and machines in e.g. biological systems or soft materials would require excitation with light that does not cause damage to the environment. To this end, various methods have been developed to redshift the excitation wavelength from UV to less destructive visible light. In 2003 it was shown that the introduction of a donor and acceptor group in the lower half allowed for photoisomerization with 435 nm.¹⁰⁵

Visible light fuelled rotation was also accomplished by triplet sensitisation (Figure 17).¹⁰⁶ Pd(TPP) possessing a long triplet lifetime and strong absorption between 500–550 nm was a suitable sensitizer for intermolecular energy transfer to the molecular motor **42**. Irradiation of the Q band of the porphyrin with 530 nm light led the successful photoisomerization of **42**, while **42** only absorbs up to 450 nm. The covalent attachment of Pd(TPP), as in motor **47**, increased the efficiency of this process considerably. Another example of visible light switching of molecular motors based on energy transfer has been reported in 2015.¹⁰⁷ Dube and co-workers designed a novel hemithioindigo based molecular motor **48** to achieve visible light driven rotation of molecular motors (Figure 18).¹⁰⁸ The introduction of a hemithioindigo moiety, originally used in photoswitches, resulted in a shift of the excitation wavelength up to 500 nm light, which offers important opportunities compared to the early 2nd generation overcrowded alkene molecular motors, which are generally fuelled with <400 nm

light. Moreover this fragment possessed other interesting features. The relative small size of the hemithioindigo allows for fast rotation and the directionality of the rotation is governed by the chirality at the sulfoxide of this hemithioindigo fragment. Hence, this fragment combines multiple functions in one and is therefore a valuable building block for future motors based on overcrowded alkenes. Higher excitation wavelengths are especially preferred in the application in a biological setting due to the deeper penetration of higher wavelength light.

Rotary molecular motors have the potential to achieve directed propulsion in aqueous solution via continuous rotational motion; an important challenge regarding the integration of molecular motors with biological function. The fundamental knowledge on how solvent properties such as viscosity affect the rotary motor is critical in achieving this goal. Several studies have been conducted on how solvent affects the THI of the rotary motors. It was found for a series of motors that the THI is retarded in media of higher viscosity. The effect is modest for non-functionalized motors,¹⁰⁹ but become increasingly pronounced, when the rotors are functionalized with larger substituents (Figure 19).¹¹⁰ A greater volume in rearranging solvent is needed with increasing substituent size, resulting in enhanced solvent displacement and consequently, retardation of the THI. Next to the size of the substituent also the rigidity plays an important role, with more rigid substituents slowing down the THI to a greater

extent. The polarity of the solvent was shown to have minimal impact on the rotational speed.

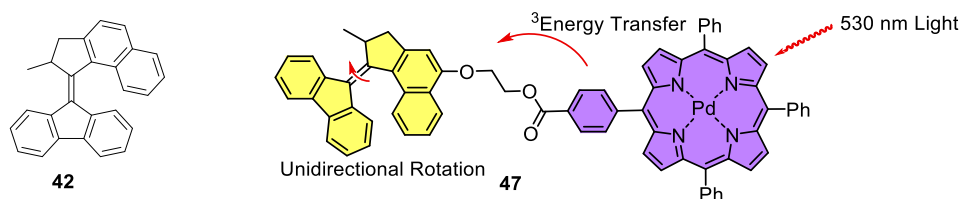


Figure 17: Visible light-driven motor **47** using energy transfer

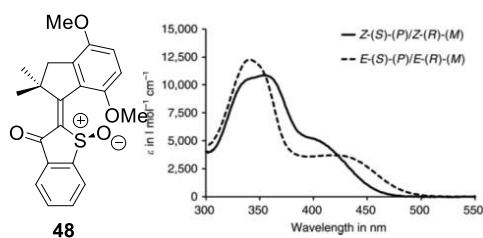


Figure 18: (Left) Hemithioindigo based molecular motor. (Right) Absorption spectra of **48**.

Next to the THI, the photochemical isomerization is also affected by increasing viscosity of the medium.¹¹¹ Studies using ultrafast spectroscopy revealed the mechanism for the photochemical isomerization. After absorption of a photon, a two-step relaxation takes place. First, one of the central carbon atoms of the alkene undergoes pyramidalization in a timeframe of about 100 femtoseconds. The second step is the torsional motion about the double bond, the power stroke of this motion which occurs on a picosecond timescale.¹¹² The pyramidalization was not affected by solvent viscosity, but the subsequent torsional motion was resisted by solvent friction and slows down by a factor of 2.5 when performed in the more viscous octanol/decalin mixture compared to acetonitrile. From these combined studies it was shown that surrounding solvent molecules influence the rotary motion of motors and that vice versa motors affect the solvent molecules. Tour and co-workers studied if the continuous rotary motion could be used to achieve motion of the molecules in solution.¹¹³ To this end various motors with different rotational speeds were equipped with fluorophores (cy5) allowing these molecules to be tracked by single molecule fluorescence correlation spectroscopy. It was found that upon irradiation, these systems exhibit increased diffusion. The largest increase in diffusion was observed for the system functionalized with the fastest motor. Since in

these experiments increased diffusion by local heating was excluded via careful control experiments and the observed correlation between increased diffusion and rotational speed, it can be concluded that the increased diffusion stems from the molecular motion of the employed motors. Although in these studies no directional motion was achieved yet, only increased diffusion, this study can be considered an important step in the development of nanomachines powered by molecular motors.

The majority of the molecular motors based on overcrowded alkenes, are fuelled by light energy. Light is a very convenient way of supplying energy to motors in solution, due to high spatiotemporal resolution one can achieve. For application of motors in e.g. surface confined or biological systems, the powering of these systems with other sources of energy such as electrical or chemical energy, would be highly beneficial. One of the challenges for the future is therefore the development of molecular motors which can be fuelled by other energy sources than light. A major hurdle to overcome in the development of electrochemically-driven molecular rotors is the chemical stability of these compounds under oxidative conditions.¹¹⁴

Almost two decades of research since the initial discovery of the light-driven unidirectional molecular rotor led to the development of large variety of molecular motors with different structure and function, and with a higher degree of control on their behaviour. The main questions which need to be addressed will be how the generated molecular motion can be translated into mesoscopic or even macroscopic directional motion and how this motion can be harnessed to achieve functions such as transport. The first steps towards answering these major questions are described in section 4.

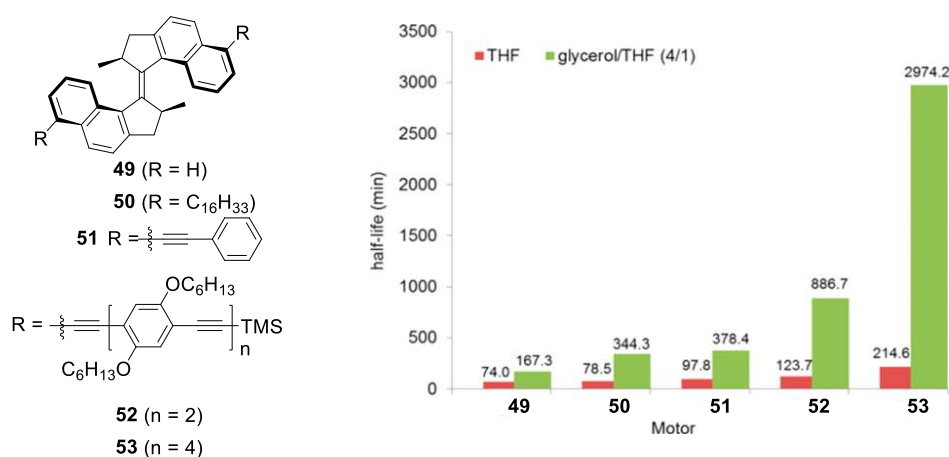


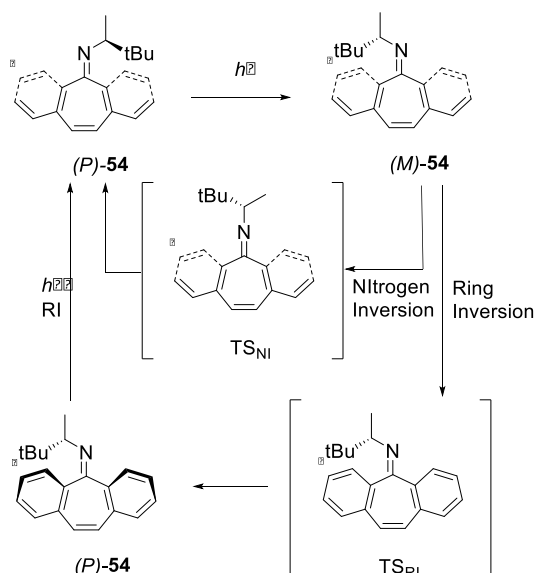
Figure 19: Molecular motors used in viscosity dependent kinetics. The $t_{1/2}$ refers to the half-life of the photogenerated metastable isomer at 25 °C.

3.5 Imines

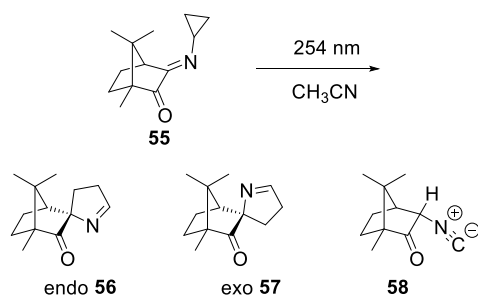
In 2006, Lehn proposed a new type of rotary molecular motor based on imine *syn-anti* isomerization.¹¹⁵ Much like alkenes, imines may undergo both photochemical and thermal isomerization. Directionality can be forced on these processes by introducing a stereogenic center close to the C=N bond. In 2014, this work resulted in the first imine-based unidirectional molecular motors.¹¹⁶ The design is based on diaryl-*N*-alkyl imines, which are stable towards thermal *E-Z* isomerization at ambient temperatures. Scheme 19 shows the structure of motor **54** and its rotational cycle. Irradiation of a diastereomeric mixture leads to photoisomerization at the C=N bond and a shift of the equilibrium towards (*M*)-**54**. The original diastereomeric ratio was restored after a thermal reaction. This thermal reaction might proceed through two different mechanism. Inversion at the nitrogen moves the substituent back to its original position. Alternatively, ring inversion of the stator can release the steric strain in (*M*)-**54**, regenerating (*P*)-**54** through an effective 180° rotation. Via the ring inversion mechanism, **54** is able to undergo a complete unidirectional 360° rotation in four steps. To distinguish between the two pathways, an asymmetric variation of **54** was synthesized. Irradiation of desymmetrized imines supports the ring inversion pathway, which means that upon irradiation and subsequent heating the compound undergoes a unidirectional 180° rotation reminiscent of the rotation of a 2nd generation overcrowded alkene-based motor.

As an alternative to this four-step 360° rotation mechanism, the barrier for ring inversion can be significantly increased by reducing the flexibility of the stator. Fusing a third benzene ring to the cycloheptene ring therefore efficiently blocks ring inversion. At higher temperatures, nitrogen inversion becomes

feasible and these compounds are shown to function as directional two-step motors. The authors note that these new motors are not only a valuable addition to the field of molecular machines, but may also be used in dynamic combinatorial chemistry, merging motional dynamics with constitutional dynamics. In a follow-up study, the authors give more details on the mechanism of the photochemical *syn-anti* isomerization of the C=N bond.¹¹⁷ This process is expected to be directional due to the placement of a stereogenic center close to the imine. Though theoretical studies confirm this assumption, experimental proof is not included in the initial study.¹¹⁶ To address this prediction, several camphor-based imines were synthesized. Camphorimine **55** (Scheme 20), bearing a cyclopropyl substituent at the nitrogen atom, undergoes both *E/Z* isomerization and photorearrangement upon irradiation with 254 nm light. Since both processes proceed through the photoinduced biradical state, the selectivity in the rearrangement is considered to be analogous to the selectivity of the isomerization. The diastereomeric ratio of *endo*-**56** and *exo*-**57** is 58:42, indicating a directional preference. The authors note that the selectivity for the biradical pathway (from the S₂ state) may be different than from the S₁ state. However, a preference of directionality was experimentally determined, completing the definite proof that chiral imines can be used as molecular motors. Since imine-based molecular motors were developed only recently, their properties remain largely unexplored. However, their potential to perform both a four-step and a two-step unidirectional 360° rotation is an intriguing addition to the existing nanomachinery toolbox. Although the principle is proven, a detailed computational and experimental study of the rotational properties is still needed to provide a thorough understanding of the mechanism. Furthermore, precise



Scheme 19: Light-induced isomerization processes of imine-based molecular motor **54**. The nitrogen inversion (NI) pathway is an effective back-and-forth switching, while the ring inversion (RI) pathway causes unidirectional 180° rotation. One hydrogen atom is marked for clarity.



Scheme 20: Camphorimine-based motor **55** and its photoproducts endo-**56**, exo-**57** and **58**.

engineering of the structure will be required to increase directional selectivity.

4. Applications

The previous sections have highlighted the translational and rotational motors available to the nanoscientist. Synthetic chemistry now holds the tools to construct systems exhibiting motion on the meso- and macroscale, which can be controlled from the molecular scale. The challenge is to convert molecular motion into function. In solution, artificial molecular motors are oriented in a random fashion. To achieve effective function, the motors need to be organized. From this organized assembly can follow both cooperativity between the motors and amplification of motion. This section will showcase some systems constructed using artificial molecular motors that allow control of dynamic function along length scales, ranging from the nanoscale to the macroscale.

4.1 Surface Functionalization

A major challenge in creating larger amplitude motion is random motion. Although the translational and rotary motion is directional, the random orientation of these molecules in solution means that the net effect of the generated motion is zero. In nature, the rotary motion of ATPase and bacterial flagella can be harnessed because they are immobilized to the cell membrane. Likewise, molecular motors can be mounted on the surface.

For rotary molecular motors, there are numerous examples of surface functionalization. The first example of a rotary molecular motor functioning while mounted on a gold nanoparticle was reported in 2005.¹¹⁸ Two connections to the surface ensured a fixed orientation of the motor, which is essential for future investigation towards cooperativity in large arrays. A combination of NMR, UV-Vis and CD studies has been used to show that the motors grafted to the surface undergo the same processes as in solution. Since then, the techniques have been refined and expanded. Molecular motors may be grafted to quartz¹¹⁹ or gold film¹²⁰, the orientation of the rotor relative to the surface can be changed from azimuthal to altitudinal,¹²¹ tetrapodal motors have been attached to the surface^{122,123} and the speed of rotation can be varied.¹²⁴ Additionally, surface bound rotary motors have been used to achieve photochemical control of surface wettability.¹²⁵ These applications illustrate the potential of surface functionalization for amplification of motor function.

Molecular switches can also be anchored to surfaces in systems exhibiting collective directional motion. In 2004, Stoddart and co-workers designed a nanomechanical device composed of microcantilever beams that undergo reversible bending in response to chemical stimuli.¹²⁶ The beams are coated with a self-assembled monolayer (SAM) of bistable [3]rotaxane **59** (Figure 20). The design of the [3]rotaxane is based on a series of bistable [2]rotaxanes switches where the position of a CBQPT⁴⁺ macrocycle can be switched between two π -electron donor recognition sites under redox conditions with excellent positional efficiency.¹²⁷ The [3]rotaxane **59** is composed of an axle bearing four π -electron donor recognition sites: two tetrathiafulvalene unit (TTF, green) and two naphthalene unit (NP, red) in an alternating order and two CBQPT⁴⁺ rings. A disulfide anchor is tethered onto each CBQPT⁴⁺, which allows the formation of a self-assembled monolayer (SAM) of **59** on gold-coated silicon cantilever array. Under neutral conditions, strong π -electron donor-acceptor interactions between the CBQPT⁴⁺ and the TTF moiety favour the positioning of the macrocycle over the TTF station. Oxidation of the TTF units to their dicationic form (TTF²⁺), disrupts this interaction and propels the macrocycle away from the TTF station onto the mildly π -electron donating

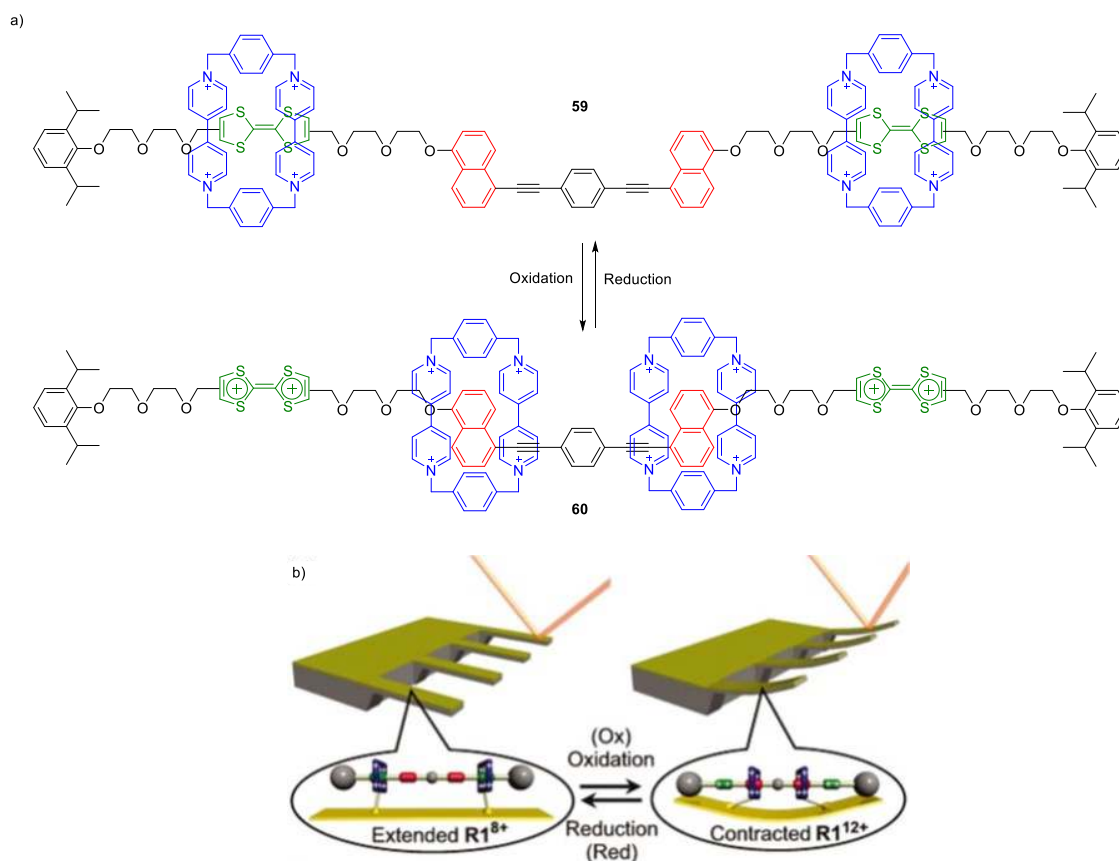


Figure 20: a) Structure of [3]rotaxane **59**. Shuttling is observed when the TTF units are oxidized (to TTF²⁺), causing repulsion between the TTF units and the macrocycles which shuttle to the NP units. The process is reversed under reductive conditions. b) Schematic representation of the contraction and relaxation of the cantilever beam. The position of the beam is measured by the deflection of an optical lever. Reproduced from Ref 126 with permission from AIP Publishing LLC, copyright 2004.

NP station in >95% efficiency (within the limits of detection by ¹H NMR spectroscopy). The shuttling of the macrocycles closer to each other contracts the surface causing a measurable ~35 nm upward mechanical bending of the beams. Reduction of the TTF²⁺ units, restores the macrocycles to their starting positions, causing the beams to relax backward. The operation cycle can be repeated up to 25 times, showing that this redox responsive system is able to perform reversible nanometer-scale mechanical work repetitively.

4.2 Unidirectional Motion at the Nanoscale

For molecular motors, the most immediately obvious application is to convert the mechanical energy into transport at the nanoscale. Nanovehicles are molecules resembling a regular car, containing wheels, axes and a chassis.¹²⁸ In theory, these may be used to transport a cargo across a surface or track. The group of Tour has synthesized numerous nanovehicles including several cars,^{129–131} a dragster,¹³² a

train,¹³³ a worm¹³⁴ and a truck¹³⁵ using spherical wheels, connected to a flat aromatic chassis *via* single and triple C-C bonds. Although these compounds are not capable of independent motion, they can be deposited on a gold surface and pushed using an STM tip.¹³¹ In 2006, the group realized a motorized version of their nanocar (Figure 21).¹³⁶ This design incorporated an overcrowded alkene-based rotary motor in the chassis. It was proposed that this motor might work as a type of propeller, moving the car over the surface with a skipping motion. The unidirectionality of the motor would enforce a directionality of the motion. The rotational properties of the motor embedded in the nanocar were studied in solution, and were found to be very similar to the parent motor.¹³⁷ In a subsequent publication, STM studies were performed to study the behaviour of motorized nanocars on a surface.¹³⁸ Although deposition on a copper surface was successful and single molecules could be imaged, no lateral motion could be induced by light or STM tip pushing, indicating

ARTICLE

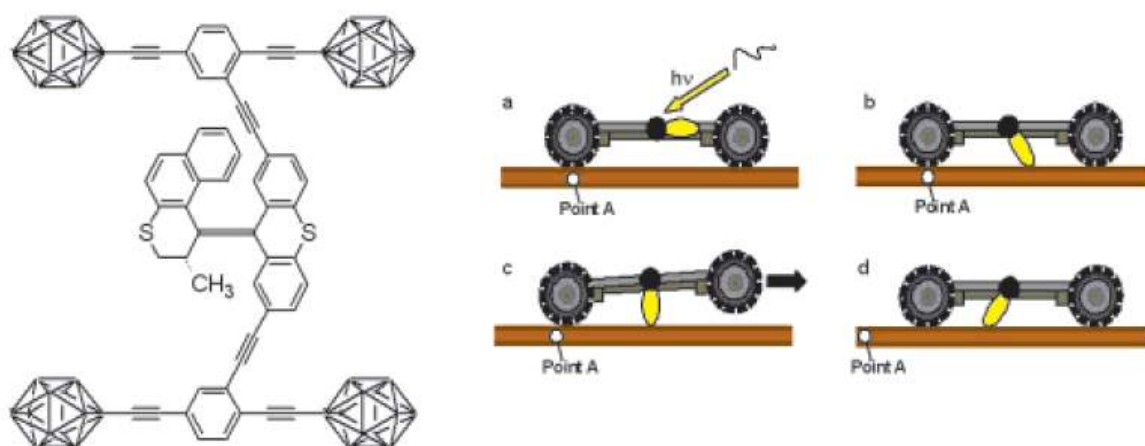


Figure 21: Nanocar by Tour *et al.* containing an overcrowded alkene-based second generation rotary molecular motor and carborane wheels. On the left, the proposed propulsion scheme is depicted: (a) the motor, depicted as a yellow blade, is irradiated with 365 nm light, leading to (b) rotation and subsequent (c,d) forward movement of the nanocar relative to the surface. Reproduced from Ref. 136 with permission from the American Chemical Society, copyright 2006.

a strong interaction between the molecule and the surface. Movement of the motorized nanocar across the surface was induced by pulses from the STM tip. Recently, Tour and co-workers demonstrated light-induced movement of a motorized 'nanoroadster' on the surface (Figure 22).¹³⁹ The roadster consists of a fast unidirectional overcrowded alkene based molecular motor attached to an axle with two adamantane wheels. At temperatures above 150K, the

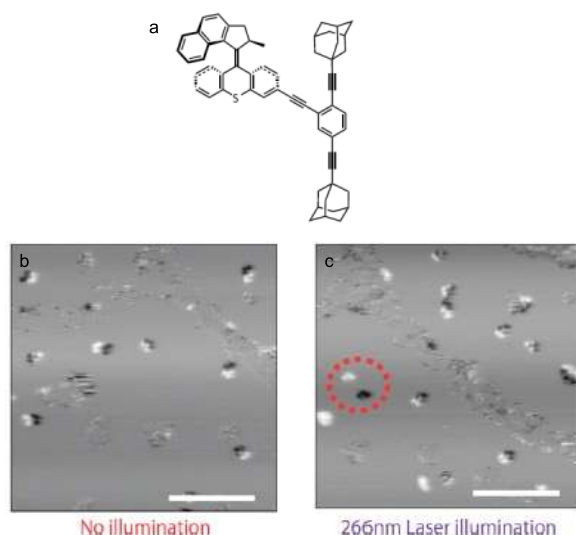


Figure 22: (a) Structure of the nanoroadster, (b) difference image of the roadsters at their starting position (dark) and after thermally induced diffusion. (white), (c) difference image of the roadsters at their starting position (dark) and after irradiation with a 266 nm laser (white).

roadsters start to diffuse across the Cu(111) surface. Irradiation causes the molecular motor to skip across the surface and increase the speed of diffusion. Although the direction of movement in these roadsters is random, this work illustrates the possibility of light-induced movement at the surface. In 2011, the group of Feringa presented the first motorized nanocar capable of directional motion across a surface.¹⁵ This design is based on a flat, aromatic chassis. However, instead of a single motor in the middle of the frame, four molecular motors are incorporated in the structure, functioning as the wheels of the car (Figure 23). In the proposed mechanism of the movement, the motors act as paddlewheels, propelling the structure forward. The nanocars could be sublimated on a copper surface and subsequently imaged using STM at 7 K. By placing the STM tip directly above the centre of an individual nanocar, a voltage could be applied and movement was induced. After 10 steps, a linear, 6 nm long trajectory was completed by a single nanocar. Although an electric voltage was used to generate motion instead of the established irradiation followed by thermal relaxation, the authors theorize that the movement is still the result of the same rotational process. This hypothesis was supported by additional STM measurements. Since the central part of the chassis consists of single and triple bonds, rotation around these bonds is possible and there is a 50% chance that the nanocar will land the wrong way (Figure 23). In the 'wrong landed' nanocar, the front and back wheels are rotating in the opposite direction. Indeed, these 'wrong landed' nanocars show no displacement upon excitation.

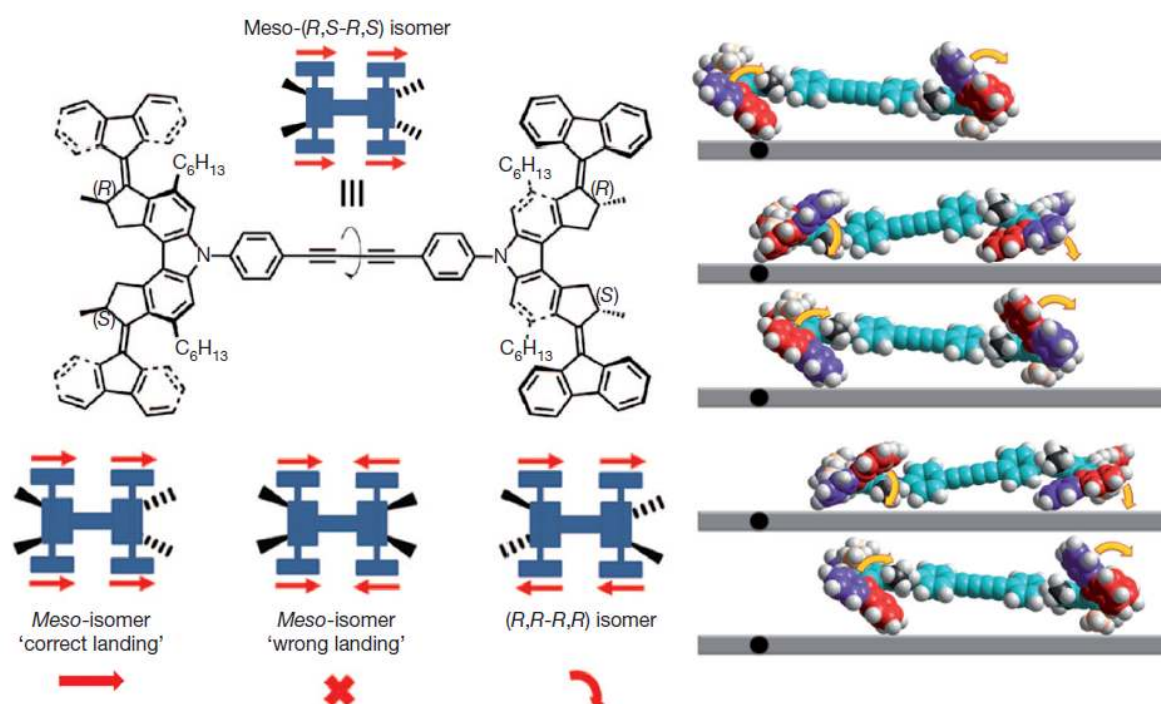


Figure 23: Motorized nanocar capable of directional movement. On the top left is depicted the Meso-(*R,S-R,S*) isomer that undergoes directional movement. Below the two 'landing modes' of the meso isomer are compared with the (*R,R-R,R*) isomer, which can only undergo circular motion. On the right is depicted a side view of the proposed mechanism of action Adapted from Ref 15. with permission from Macmillan Publishers Limited, copyright 2011.

Moreover, the *R,R-R,R* diastereomer of the nanocar was synthesized, in which the combination of stereocenters was expected to lead to circular movement. STM measurements of these diastereomers indeed showed a random trajectory. The synthesis of the four-wheeled motorized nanocar required 13 synthetic steps and chiral HPLC separation, with an overall yield of 1.3%. As these values indicate, conventional synthetic chemistry is reaching its practical limit here. Therefore, for larger scale applications, chemists need to rely on other methods, such as cooperativity between clusters and amplification of motion. From a practical point of view this most likely means systems based on supramolecular assemblies, polymer chemistry or surface functionalization.

4.3 Unimolecular Motion at the Microscale

Besides surface functionalization, other approaches towards amplification of motion exist. In 2006, Feringa and co-workers used an alkene-based rotary molecular motor to rotate a 5x28 μm glass rod.¹⁴⁰ A cholesteric liquid crystal film was doped with 1 wt% of an enantiopure second generation motor (Figure 24a). As mentioned previously, the central structure of these motors is helical, and every step in the rotary process is accompanied by a change in helicity. When the motor is used

as a dopant, the liquid crystal adopts the same helicity through a 'sergeants-and-soldiers' principle.¹⁴¹ When the sample is irradiated, the helicity of the dopant changes, leading to a rearrangement of the liquid crystal (Figure 24 b-e). This rearrangement occurs in a clockwise fashion. A microscopic glass rod, deposited on top of the LC layer was used to visualize this movement. Irradiation with 365 nm light caused the rod to rotate in a clockwise manner. After 10 min, the movement gradually halted, but resumed again in an anti-clockwise direction upon removal of the irradiation source. A control experiment using the opposite enantiomer induced rotation in the opposite direction. The rotation of the glass is a direct result of the switching helicity of the dopant, rather than the unidirectionality of the rotation of the motor. However, the transfer of motion from nanoscopic motors to a small glass rod that is visible with an optical microscope is a definitive landmark in the development and application of artificial molecular motors. However, nanoscopically induced macroscopic motion remains the Holy Grail in molecular motors research. Two pertinent examples will be discussed in the following section.

4.4 Unimolecular Motion at the Macroscale

Leigh and co-workers used the shuttling of a macrocycle to directionally transport a droplet along a photo-responsive surface functionalized with bistable rotaxane **61**¹⁴², related to the photoswitchable surface wettability later reported by Feringa and co-workers.¹²⁵ The stimuli-responsive molecular shuttle **61** is able to expose or conceal a fluoroalkane segment depending on the position of the macrocycle. They had shown previously that the macrocycle can discriminate between three binding moieties in the order fumaramide>succinamide>maleamide.¹⁴³ The contact angle of polar liquids on a surface is known to deviate as a function of the polarophilicity of the surface. By incorporating polarophobic fluoroalkane groups into the succinamide station, the system can affect the contact angle of polar liquids with a shuttle-coated surface. To begin, the macrocycle preferentially resides over the fumaramide station (>95%) leaving the polarophobic fluoro-succinamide motif exposed. Irradiation of the surface results in *E* to *Z* isomerization of the olefin to the maleamide which has lower binding affinity for the macrocycle, driving it away from this station onto the now higher-affinity succinamide station, thus concealing the polarophobic group to create a more polarophilic surface. As a result, the affinity with the polar liquid droplets increases as indicated by the significant decrease in the contact angles. This effect was used to directionally transport a diiodomethane drop across the surface. Focusing the irradiation on one side of the drop (right-hand side, Figure 25b) and the adjacent area, decreases the contact angle of the droplet within the irradiated area, while the contact angle with the non-irradiated area remains the same. The disparity between the contact angles creates a pressure gradient inside the droplet, causing it to elongate and advance towards the more polarophilic area of the surface. After 580 s of

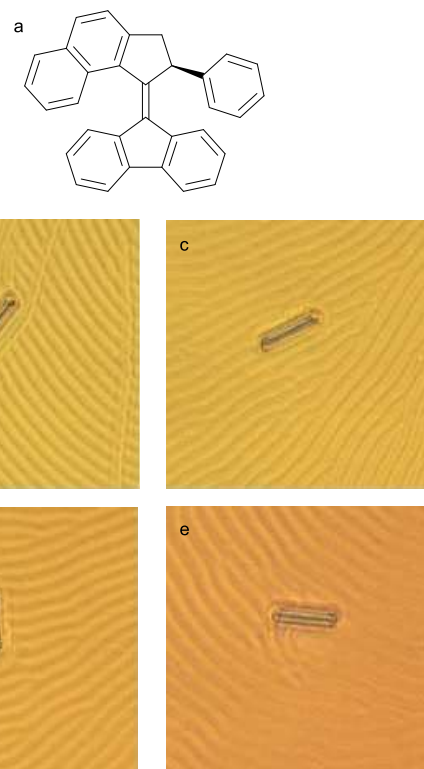


Figure 24: Unidirectional rotation of a macroscopic glass rod. (a) Structure of the molecular motor dopant. (b) Initial orientation of glass rod on LC surface, (c) after 15 s of irradiation, the glass rod has rotated 28° with respect to its original position, (d) 30 s, 141°, (e) 45 s, 226°. Reproduced from Ref. 140 with permission from Macmillan Publishers Ltd, copyright 2006.

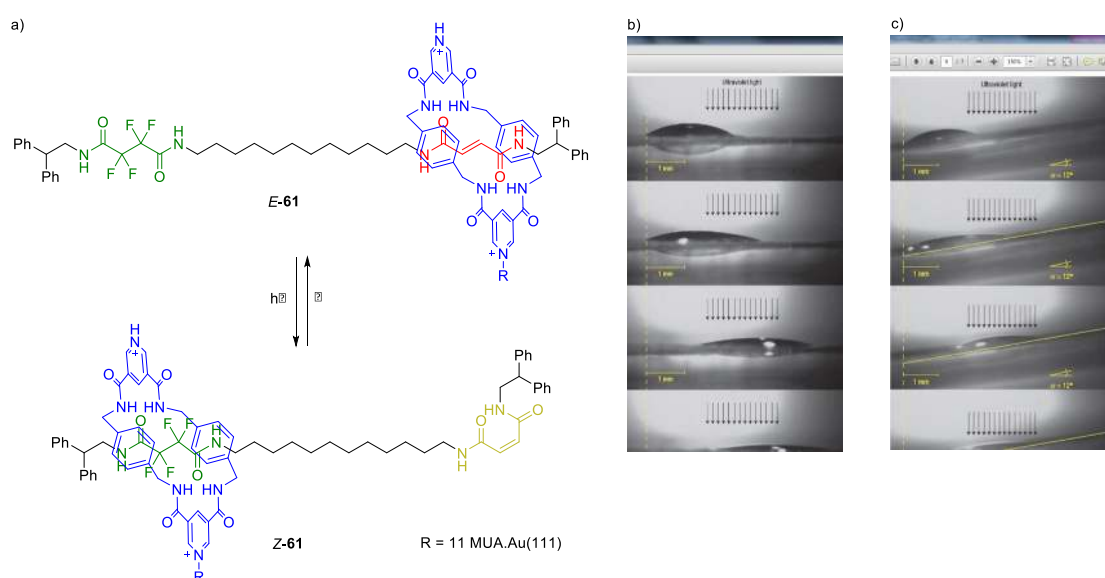


Figure 25. (a) Structure of photo-responsive shuttle **61**. Shuttling is observed when the fumaramide station is isomerized to the maleamide (*E*-**61**:*Z*-**61** is 50:50 at the photostationary state). Thermal relaxation re-establishes the starting distribution. (b) Lateral photographs of light-driven transport of a diiodomethane droplet on a surface of **61** on mica. The arrows show the irradiated area. Photographs were taken (top to bottom) before irradiation, after 215 s, 370 s and 580 s of irradiation. (c) Lateral photographs of light-driven transport of a diiodomethane droplet on a surface of **61** on mica on a 12° incline. The arrows show the irradiated area. Photographs were taken (top to bottom) before irradiation, after 160 s, 245 s and 640 s of irradiation. Reproduced from Ref. 142 with permission from Macmillan Publishers Ltd, copyright 2005.

ARTICLE

irradiation, the diiodomethane droplet (1.25 μL) has been directionally transported by 1.5 mm along the mica surface. Leigh and co-workers were also able to induce unidirectional macroscopic transport of the droplet against the force of gravity on a 12° inclined surface (Figure 25) demonstrating that mechanical motion at the molecular level can be translated into macroscopic transport. However, the shuttle on which this system is based cannot be classed as a motor as the macrocycle can access both stations at equilibrium through Brownian motion (see Section 1). Photo-isomerisation simply changes the position of the equilibrium and the removal of the stimulus restores the original distribution. However, the collective action of the monolayer of rotaxane shuttles acts as a motor, transporting the diiodomethane droplet to a position that it cannot access through Brownian motion.

Giuseppone and co-workers¹⁴⁴ have developed a polymeric gel including 2nd generation overcrowded alkene based molecular motors, which contracts upon irradiation with UV light. The polymer motor conjugates were synthesized using conventional Huisgen click chemistry¹⁴⁵ and consist of fast (MHz) second generation motors crosslinked with PEG chains. The polymer forms a gel in 10 wt% toluene. A piece of this gel, suspended in toluene, was shown to contract visibly upon irradiation with UV light. It is hypothesized that this shrinking is the result of increasingly tighter coiling of the polymeric chains, induced by the continuous rotation of the motor units. At higher tensions the contraction slows down, until the gels ruptures and subsequently recovers its original size and shape. Complimentary fluorescence experiments indicate that the rupture is the result of simultaneous oxidation of the central double bonds of the motors, followed by unwinding of the coils. AFM analysis of smaller pieces of gel supports the coiling hypothesis, since pores in the compacted gel are stretched out to over twice their original size, and shrink again after rupture. The authors imagine these systems may be of use in energy storage, but many more potential applications spring to mind readily, including smart materials and artificial muscles. This research is an excellent example of translating molecular motion into macroscopic function and moreover, an impressive illustration of the power of molecular machines.

5. Conclusions

The potential of nanotechnology was first predicted by Feynman in his visionary lecture 'There is plenty of room at the bottom'.¹⁴⁶ Although he envisioned nanotechnology to be approached top down, synthetic chemists embarked on a bottom-up journey, exploring the possibilities to achieve

directional movement at a length scale where Brownian motion is dominant. In the last decades, a multitude of molecular motors have been developed. In this review we have shown how molecular motors have evolved from elegant proof-of-principles to advanced designs, capable of repetitive and directional motion at the nanoscale. The development of these systems holds great promise for applications in the field of nanotechnology, but also raises key questions on the fundamental difference between the macroscopic and molecular world and how to address these issues in designing functional molecular motors. It is extraordinary to realize how fast this field has progressed from being basically non-existent a quarter century ago, up till now, where control of motion and function at the nanoscale lie within the grasp of chemists' hands. Focusing on the predominant classes of molecular motors, i.e. molecular walkers, rotaxane and catenane based systems and covalently bonded motors, it can be said that major steps have been taken in their design and synthesis. However, formidable challenges remain. Recent focus of research on these systems lies on the improvement of the performance and achieving additional means of control. Since control of directional molecular motion is achieved and understood to a large extent, the main question remains is how to convert this motion into useful functionality? In this review several examples are given of how these motors can be incorporated into systems able to perform useful work. It is beautiful to see that the action of these motors can achieve the tiniest motion at the nanoscale via contraction of cantilevers and rotation of microrods, up to the macroscopic movement of droplets or gels. Nevertheless, when it comes to function, artificial molecular motors currently pale in comparison to the motors found in Nature. However it should be remembered that Nature has had a head start of several billion years, while nanoscientists have only just started to uncover the fledgling potential of nanotechnology. We have no doubt that time will reveal remarkable possibilities for artificial molecular motors.

Acknowledgements

We gratefully acknowledge generous support from NanoNed, The Netherlands Organization for Scientific Research (NWO-CW Top grant to BLF), the Royal Netherlands Academy of Arts and Sciences (KNAW), the Ministry of Education, Culture and Science (Gravitation programme 0024.001.0035), the Engineering and Physical Sciences Research Council (EPSRC), the Royal Society and the European Research Council (Advanced Investigator Grants no. 694345 to BLF and no 339019 to DAL). MRW thanks the Novo Nordisk STAR

programme for a postdoctoral fellowship. We thank dr. S. J. Wezenberg for valuable discussions.

Notes and references

- 1 M. A. Hoyt, A. A. Hyman and M. Baehler, *Proc. Natl. Acad. Sci.*, 1997, **94**, 12747.
- 2 H. Lodish, A. Berk, S. L. Zipursky, P. Matsudaira, D. Baltimore and J. Darnell, *Molecular Cell Biology*, 4th edition, W. H. Freeman, New York 2000.
- 3 B. Alberts, A. Johnson, J. Lewis, M. Raff, K. Roberts and P. Walter, *Molecular Biology of the Cell*, 4th edition, Garland Science, New York 2002.
- 4 C. Mavroidis, A. Dubey and M. L. Yarmush, *Annu. Rev. Biomed. Eng.*, 2004, **6**, 363.
- 5 L. A. Amos, *Cell. Mol. Life Sci.*, 2008, **65**, 509.
- 6 M. Schliwa and G. Woehlke, *Nature*, 2003, **422**, 759.
- 7 K. Kinbara and T. Aida, *Chem. Rev.*, 2005, **105**, 1377.
- 8 P. D. Boyer, *Nature*, 1999, **402**, 247.
- 9 M. Schliwa, *Molecular motors*, Wiley-VCH, Weinheim, 2003.
- 10 R. D. Vale, *Cell*, **2003**, 112, 467.
- 11 R. D. Vale and R. A. Milligan, *Science*, 2000, **288**, 88.
- 12 T. R. Kelly, M. C. Bowyer, K. V. Bhaskar, D. Bebbington, A. Garcia, F. Lang, M. H. Kim and M. P. Jette, *J. Am. Chem. Soc.*, 1994, **116**, 3657.
- 13 J. D. Badjić, V. Balzani, A. Credi, S. Silvi and J. F. Stoddart, *Science*, 2004, **303**, 1845.
- 14 M. C. Jiménez, C. Dietrich-Buchecker and J.-P. Sauvage, *Angew. Chem. Int. Ed.*, 2000, **39**, 3284.
- 15 T. Kudernac, N. Ruangsapapichat, M. Parschau, B. Maciá, N. Katsonis, S. R. Harutyunyan, K.-H. Ernst and B. L. Feringa, *Nature*, 2011, **479**, 208.
- 16 P. L. Anelli, N. Spencer and J. F. Stoddart, *J. Am. Chem. Soc.*, 1991, **113**, 5131.
- 17 S. Silvi, M. Venturi and A. Credi, *J. Mater. Chem.*, 2009, **19**, 2279.
- 18 M. N. Chatterjee, E. R. Kay and D. A. Leigh, *J. Am. Chem. Soc.*, 2006, **128**, 4058.
- 19 V. Serreli, C.-F. Lee, E. R. Kay and D. A. Leigh, *Nature*, 2007, **445**, 523.
- 20 M. Alvarez-Pérez, S. M. Goldup, D. A. Leigh and A. M. Z. Slawin, *J. Am. Chem. Soc.*, 2008, **130**, 1836.
- 21 A. Carlone, S. M. Goldup, N. Lebrasseur, D. A. Leigh and A. Wilson, *J. Am. Chem. Soc.*, 2012, **134**, 8321.
- 22 B. Lewandowski, G. De Bo, J. W. Ward, M. Papmeyer, S. Kuschel, M. J. Aldegunde, P. M. E. Gramlich, D. Heckmann, S. M. Goldup, D. M. D'Souza, A. E. Fernandes and D. A. Leigh, *Science*, 2013, **339**, 189.
- 23 G. De Bo, S. Kuschel, D. A. Leigh, B. Lewandowski, M. Papmeyer and J. W. Ward, *J. Am. Chem. Soc.*, 2014, **136**, 5811.
- 24 S. Kassem, A. T. L. Lee, D. A. Leigh, A. Markevicius and J. Solà, *Nature Chem.*, 2016, **8**, 138.
- 25 M. von Delius and D. A. Leigh, *Chem. Soc. Rev.*, 2011, **40**, 3656.
- 26 D. A. Leigh, U. Lewandowska, B. Lewandowski and M. R. Wilson, *Top. Curr. Chem.*, 2014, **354**, 111.
- 27 a) W. R. Browne, B. L. Feringa, *Nature Nanotech.*, 2006, **1**, 25. b) B. L. Feringa, *J. Org. Chem.*, 2007, **72**, 6635. c) *From Non-Covalent Assemblies to Molecular Machines*, ed. J. P. Sauvage and P. Gaspard, Wiley-VCH, Weinheim, 2010. d) V. Balzani, A. Credi and M. Venturi, *Molecular Devices and Machines: Concepts and Perspectives for the Nanoworld*, Wiley-VCH, Weinheim, 2nd edition, 2008. e) S. Erbas-Cakmak, D. A. Leigh, C. T. McTernan and A. L. Nussbaumer, *Chem. Rev.*, 2015, **115**, 10081. f) C. J. Bruns, J. F. Stoddart, *The Nature of the Mechanical Bond: From Molecules to Machines*, John Wiley and Sons, Hoboken, 2016. g) R. D. Astumian, *Chem. Sci.*, 2017, **8**, 840. h) C. Pezzato, C. Cheng, J. F. Stoddart, R. D. Astumian, *Chem. Soc. Rev.*, 2017, asap.
- 28 R. D. Astumian, *Phys. Chem. Chem. Phys.*, 2007, **9**, 5067.
- 29 H. Gu, J. Chao, S.-J. Xiao and N. C. Seeman, *Nature*, 2010, **465**, 202.
- 30 J.-S. Shin and N. A. Pierce, *J. Am. Chem. Soc.*, 2004, **126**, 10834.
- 31 K. Lund, A. J. Manzo, N. Dabby, N. Michelotti, A. Johnson-Buck, J. Nangreave, S. Taylor, R. Pei, M. N. Stojanovic, N. G. Walter, E. Winfree and H. Yan, *Nature*, 2010, **465**, 206.
- 32 W. B. Sherman and N. C. Seeman, *Nano Lett.*, 2004, **4**, 1203.
- 33 P. Yin, H. Yan, X. G. Daniell, A. J. Turberfield and J. H. Reif, *Angew. Chem. Int. Ed.*, 2004, **43**, 4906.
- 34 J. Bath, S. J. Green and A. J. Turberfield, *Angew. Chem. Int. Ed.*, 2005, **44**, 4358.
- 35 Y. Tian, Y. He, Y. Chen, P. Yin and C. Mao, *Angew. Chem. Int. Ed.*, 2005, **44**, 4355.
- 36 S. J. Green, J. Bath and A. J. Turberfield, *Phys. Rev. Lett.*, 2008, **101**, 238101.
- 37 P. Yin, H. M. T. Choi, C. R. Calvert and N. A. Pierce, *Nature*, 2008, **451**, 318.
- 38 T. Omabegho, R. Sha and N. C. Seeman, *Science*, 2009, **324**, 67.
- 39 W. Sherman, *Science*, 2009, **324**, 46.
- 40 Y. He and D. R. Liu, *Nat. Nanotechnol.*, 2010, **5**, 778.
- 41 M. von Delius, E. M. Geertsema and D. A. Leigh, *Nature Chem.*, 2010, **2**, 96.
- 42 M. von Delius, E. M. Geertsema, D. A. Leigh, D.-T. D. Tang, *J. Am. Chem. Soc.*, 2010, **132**, 16134.
- 43 E. R. Kay, D. A. Leigh and F. Zerbetto, *Angew. Chem. Int. Ed.*, 2007, **46**, 72.
- 44 M. J. Barrell, A. G. Campaña, M. von Delius, E. M. Geertsema and D. A. Leigh, *Angew. Chem. Int. Ed.*, 2011, **50**, 285.
- 45 A. G. Campaña, A. Carlone, K. Chen, D. T. F. Dryden, D. A. Leigh, U. Lewandowska and K. M. Mullen, *Angew. Chem. Int. Ed.*, 2012, **51**, 5480.
- 46 A. G. Campaña, D. A. Leigh and U. Lewandowska, *J. Am. Chem. Soc.*, 2013, **135**, 8639.
- 47 P. Kovaříček and J.-M. Lehn, *J. Am. Chem. Soc.*, 2012, **134**, 9446.
- 48 P. Kovaříček and J.-M. Lehn, *Chem. Eur. J.*, 2015, **21**, 9380.
- 49 J. E. Beves, V. Blanco, B. A. Blight, R. Carrillo, D. M. D'Souza, D. Howgego, D. A. Leigh, A. M. Z. Slawin and M. D. Symes, *J. Am. Chem. Soc.*, 2014, **136**, 2094.
- 50 E. R. Kay and D. A. Leigh, *Pure Appl. Chem.*, 2008, **80**, 17.
- 51 C. Dietrich-Buchecker, M. C. Jimenez-Molero, V. Sartor and J.-P. Sauvage, *Pure Appl. Chem.*, 2003, **75**, 1383.
- 52 I. T. Harrison and S. Harrison, *J. Am. Chem. Soc.*, 1967, **89**, 5723.
- 53 E. Wasserman, *J. Am. Chem. Soc.*, 1960, **82**, 4433.
- 54 A. S. Lane, D. A. Leigh and A. Murphy, *J. Am. Chem. Soc.*, 1997, **119**, 11092.
- 55 R. A. Bissell, E. Córdova, A. E. Kaifer and J. F. Stoddart, *Nature*, 1994, **369**, 133.
- 56 M. Baroncini, S. Silvi, M. Venturi and A. Credi, *Angew. Chem.*

- Int. Ed.*, 2012, **51**, 4223.
- 57 G. Ragazzon, M. Baroncini, S. Silvi, M. Venturi and A. Credi, *Nat. Nanotechnol.*, 2014, **10**, 70.
- 58 H. Li, C. Cheng, P. R. McGonigal, A. C. Fahrenbach, M. Frascioni, W.-G. Liu, Z. Zhu, Y. Zhao, C. Ke, J. Lei, R. M. Young, S. M. Dyar, D. T. Co, Y.-W. Yang, Y. Y. Botros, W. A. Goddard III, M. R. Wasielewski, R. D. Astumian and J. F. Stoddart, *J. Am. Chem. Soc.*, 2013, **135**, 18609.
- 59 C. Cheng, P. R. McGonigal, W.-G. Liu, H. Li, N. A. Vermeulen, C. Ke, M. Frascioni, C. L. Stern, W. A. Goddard III and J. F. Stoddart, *J. Am. Chem. Soc.*, 2014, **136**, 14702.
- 60 C. Cheng, P. R. McGonigal, S. T. Schneebeli, H. Li, N. A. Vermeulen, C. Ke and J. F. Stoddart, *Nat. Nanotechnol.*, 2015, **10**, 547.
- 61 a) A. Livoreil, C. O. Dietrich-Buchecker, J.-P. Sauvage, *J. Am. Chem. Soc.*, 1994, **116**, 9399. b) F. Baumann, A. Livoreil, W. Kaim, J.-P. Sauvage, *Chem. Commun.*, 1997, 35. c) A. Livoreil, J.-P. Sauvage, N. Armaroli, V. Balzani, L. Flamigni, B. Ventura, *J. Am. Chem. Soc.*, 1997, **119**, 12114.
- 62 D. J. Cardenas, A. Livoreil, J.-P. Sauvage, *J. Am. Chem. Soc.*, 1996, **118**, 11980.
- 63 D. A. Leigh, J. K. Y. Wong, F. Dehez and F. Zerbetto, *Nature*, 2003, **424**, 174.
- 64 J. V. Hernández, E. R. Kay and D. A. Leigh, *Science*, 2004, **306**, 1532.
- 65 M. R. Wilson, J. Solà, A. Carlone, S. M. Goldup, N. Lebrasseur and D. A. Leigh, *Nature*, 2016, **534**, 235.
- 66 T. R. Kelly, I. Tellitu and J. P. Sestelo, *Angew. Chem. Int. Ed.*, 1997, **36**, 1866.
- 67 T. R. Kelly, J. P. Sestelo and I. Tellitu, *J. Org. Chem.*, 1998, **63**, 3655.
- 68 T. R. Kelly, H. De Silva and R. A. Silva, *Nature*, 1999, **401**, 150.
- 69 T. R. Kelly, R. A. Silva, H. De Silva, S. Jasmin and Y. Zhao, *J. Am. Chem. Soc.*, 2000, **122**, 6935.
- 70 A. P. Davis, *Angew. Chem. Int. Ed.*, 1998, **37**, 909.
- 71 T. R. Kelly, *Acc. Chem. Res.*, 2001, **34**, 514.
- 72 T. R. Kelly, X. Cai, F. Damkaci, S. B. Panicker, B. Tu, S. M. Bushell, I. Cornella, M. J. Piggott, R. Salives, M. Caverio, Y. Zhao and S. Jasmin, *J. Am. Chem. Soc.*, 2007, **129**, 376.
- 73 W. L. Mock and K. J. Ochwat, *J. Phys. Org. Chem.*, 2003, **16**, 175.
- 74 G. Haberhauer, *Angew. Chem. Int. Ed.*, 2011, **50**, 6415.
- 75 G. Bringmann, A. J. P. Mortimer, P. A. Keller, M. J. Gresser, J. Garner and M. Breuning, *Angew. Chem. Int. Ed.*, 2005, **44**, 5384.
- 76 B. J. Dahl and B. P. Branchaud, *Tetrahedron Lett.*, 2004, **45**, 9599.
- 77 Y. Lin, B. J. Dahl and B. P. Branchaud, *Tetrahedron Lett.*, 2005, **46**, 8359.
- 78 B. J. Dahl and B. P. Branchaud, *Org. Lett.*, 2006, **8**, 5841.
- 79 S. P. Fletcher, F. Dumur, M. M. Pollard and B. L. Feringa, *Science*, 2005, **310**, 80.
- 80 N. Koumura, R. W. Zijlstra, R. A. van Delden, N. Harada and B. L. Feringa, *Nature*, 1999, **401**, 152.
- 81 B. S. L. Collins, J. C. M. Kistemaker, E. Otten and B. L. Feringa, *Nature Chem.*, 2016, **8**, 860.
- 82 H. L. Tierney, C. J. Murphy, A. D. Jewell, A. E. Baber, E. V. Iski, H. Y. Khodaverdian, A. F. McGuire, N. Klebanov and E. C. H. Sykes, *Nat. Nanotechnol.*, 2011, **6**, 625.
- H. L. Tierney, C. J. Murphy and E. C. H. Sykes, *Phys. Rev. Lett.*, 2011, **106**, 1.
- N. Koumura, E. M. Geertsema, A. Meetsma and B. L. Feringa, *J. Am. Chem. Soc.*, 2000, **122**, 12005.
- J. C. M. Kistemaker, P. Štacko, J. Visser and B. L. Feringa, *Nat. Chem.*, 2015, **7**, 890.
- R. S. Cahn, C. Ingold and V. Prelog, *Angew. Chem. Int. Ed.*, 1966, **5**, 385.
- V. Prelog and G. Helmchen, *Angew. Chem. Int. Ed.*, 1982, **21**, 567.
- J. C. M. Kistemaker, S. F. Pizzolato, T. van Leeuwen, T. C. Pijper and B. L. Feringa, *Chem. Eur. J.*, 2016, **22**, 13478.
- N. Ruangsapapichat, M. M. Pollard, S. R. Harutyunyan and B. L. Feringa, *Nature Chem.*, 2011, **3**, 53.
- R. A. van Delden, M. K. J. ter Wiel, H. de Jong, A. Meetsma and B. L. Feringa, *Org. Biomol. Chem.*, 2004, **2**, 1531.
- D. H. Qu and B. L. Feringa, *Angew. Chem. Int. Ed.*, 2010, **49**, 1107.
- R. Augulis, M. Klok, B. L. Feringa and P. H. M. Van Loosdrecht, *Phys. Stat. Sol. C*, 2009, **6**, 181.
- J. Vicario, M. Walko, A. Meetsma and B. L. Feringa, *J. Am. Chem. Soc.* 2006, **128**, 5127.
- J. Vicario, A. Meetsma, B. L. Feringa, *Chem. Comm.*, 2005, 5910.
- T. Fernández Landaluce, G. London, M. M. Pollard, P. Rudolf and B. L. Feringa, *J. Org. Chem.*, 2010, **75**, 5323.
- M. M. Pollard, A. Meetsma and B. L. Feringa, *Org. Biomol. Chem.*, 2008, **6**, 507.
- E. M. Geertsema, N. Koumura, M. K. J. ter Wiel, A. Meetsma and B. L. Feringa, *Chem. Commun.*, 2002, 2962.
- G. Pérez-Hernández and L. González, *Phys. Chem. Chem. Phys.*, 2010, **12**, 12279.
- M. Klok, N. Boyle, M. T. Pryce, A. Meetsma, W. R. Browne and B. L. Feringa, *J. Am. Chem. Soc.*, 2008, **130**, 10484.
- B. Oruganti, C. Fang and B. Durbreej, *Phys. Chem. Chem. Phys.*, 2015, **17**, 21740.
- A. Faulkner, T. van Leeuwen, B. L. Feringa and S. J. Wezenberg, *J. Am. Chem. Soc.*, **138**, 13597.
- M. M. Pollard, P. V. Wesenhagen, D. Pijper and B. L. Feringa, *Org. Biomol. Chem.*, 2008, **6**, 1605.
- D. Pijper, R. A. Van Delden, A. Meetsma and B. L. Feringa, *J. Am. Chem. Soc.*, 2005, **127**, 17612.
- B. Oruganti and B. Durbreej, *J. Mol. Model.*, 2016, **22**, 38.
- R. A. van Delden, N. Koumura, A. Schoevaars, A. Meetsma and B. L. Feringa, *Org. Biomol. Chem.*, 2003, **1**, 33.
- A. Cnossen, L. Hou, M. M. Pollard, P. V. Wesenhagen, W. R. Browne and B. L. Feringa, *J. Am. Chem. Soc.*, 2012, **134**, 17613.
- S. J. Wezenberg, K. Y. Chen and B. L. Feringa, *Angew. Chem. Int. Ed.*, 2015, **54**, 11457.
- M. Guentner, M. Schildhauer, S. Thumser, P. Mayer, D. Stephenson, P. J. Mayer and H. Dube, *Nat. Commun.*, 2015, **6**, 8406.
- J. C. M. Kistemaker, A. S. Lubbe, E. A. Bloemsmas and B. L. Feringa, *ChemPhysChem*, 2016, 1819.
- J. Chen, J. C. M. Kistemaker, J. Robertus and B. L. Feringa, *J.*

- Am. Chem. Soc.*, 2014, **136**, 14924.
- 111 J. Conyard, A. Cnossen, W. R. Browne, B. L. Feringa and S. R. Meech, *J. Am. Chem. Soc.*, 2014, **136**, 9692.
- 112 J. Conyard, K. Addison, I. A. Heisler, A. Cnossen, W. R. Browne, B. L. Feringa and S. R. Meech, *Nature Chem.*, 2012, **4**, 547.
- 113 V. García-López, P. T. Chiang, F. Chen, G. Ruan, A. A. Martí, A. B. Kolomeisky, G. Wang and J. M. Tour, *Nano Lett.*, 2015, **15**, 8229.
- 114 H. Logtenberg, J. Areephong, J. Bauer, A. Meetsma, B. L. Feringa and W. R. Browne, *ChemPhysChem*, 2016, 1895.
- 115 J.-M. Lehn, *Chem. Eur. J.*, 2006, **12**, 5910.
- 116 L. Greb and J.-M. Lehn, *J. Am. Chem. Soc.*, 2014, **136**, 13114.
- 117 L. Greb, A. Eichhöfer and J.-M. Lehn, *Angew. Chem. Int. Ed.*, 2015, **54**, 14345.
- 118 R. A van Delden, M. K. J. ter Wiel, M. M. Pollard, J. Vicario, N. Koumura and B. L. Feringa, *Nature*, 2005, **437**, 1337.
- 119 M. M. Pollard, M. Lubomska, P. Rudolf and B. L. Feringa, *Angew. Chem. Int. Ed.*, 2007, **46**, 1278.
- 120 G. T. Carroll, M. M. Pollard, R. A. van Delden and B. L. Feringa, *Chem. Sci.*, 2010, **1**, 97.
- 121 G. London, G. T. Carroll, T. Fernández Landaluce, M. M. Pollard, P. Rudolf and B. L. Feringa, *Chem. Comm.* 2009, 1712.
- 122 K. -Y. Chen, S. J. Wezenberg, G. T. Carroll, G. London, J. C. M. Kistemaker, T. C. Pijper and B. L. Feringa, *J. Org. Chem.*, 2014, **79**, 7032.
- 123 J. Chen, K.-Y. Chen, G. T. Carroll and B. L. Feringa, *Chem. Comm.*, 2014, **50**, 12641.
- 124 J. Vachon, G. T. Carroll, M. M. Pollard, E. M. Mes, A. M. Brouwer and B. L. Feringa, *Photochem. Photobiol. Sci.*, 2014, **13**, 241.
- 125 K. -Y. Chen, O. Ivashenko, G. T. Carroll, J. Robertus, J. C. M. Kistemaker, G. London, W. R. Browne, P. Rudolf and B. L. Feringa, *J. Am. Chem. Soc.*, 2014, **136**, 3219.
- 126 T. J. Huang, B. Brough, C.-M. Ho, Y. Liu, A. H. Flood, P. A. Bonvallet, H.-R. Tseng, J. F. Stoddart, M. Baller and S. Magonov, *Appl. Phys. Lett.*, 2004, **85**, 5391.
- 127 H. R. Tseng, S. A. Vignon and J. F. Stoddart, *Angew. Chem. Int. Ed.*, 2003, **42**, 149.
- 128 Y. Shirai, J.-F. Morin, T. Sasaki, J. M. Guerrero and J. M. Tour, *Chem. Soc. Rev.*, 2006, **35**, 1043.
- 129 T. Sasaki and J. M. Tour, *Tetrahedron Lett.*, 2007, **48**, 5821.
- 130 T. Sasaki, A. J. Osgood, L. B. Alemany, K. F. Kelly and J. M. Tour, *Org. Lett.*, 2008, **10**, 229.
- 131 Y. Shirai, A. J. Osgood, Y. Zhao, K. F. Kelly and J. M. Tour, *Nano Lett.*, 2005, **5**, 2330.
- 132 G. Vives, J. Kang, K. F. Kelly and J. M. Tour, *Org. Lett.*, 2009, **11**, 5602.
- 133 T. Sasaki, J. M. Guerrero, A. D. Leonard and J. M. Tour, *Nano Res.* 2008, **1**, 412.
- 134 T. Sasaki and J. M. Tour, *Org. Lett.*, 2008, **10**, 897.
- 135 T. Sasaki, J. F. Morin, M. Lu and J. M. Tour, *Tetrahedron Lett.*, 2007, **48**, 5817.
- 136 J. F. Morin, Y. Shirai and J. M. Tour, *Org. Lett.*, 2006, **8**, 1713.
- 137 N. Koumura, E. M. Geertsema, M. B. Van Gelder, A. Meetsma and B. L. Feringa, *J. Am. Chem. Soc.*, 2002, **124**, 5037.
- 138 P. T. Chiang, J. Mielke, J. Godoy, J. M. Guerrero, L. B. Alemany, C. J. Villagómez, A. Saywell, L. Grill and J. M. Tour, *ACS Nano*, 2012, **6**, 592.
- 139 A. Saywell, A. Bakker, J. Mielke, T. Kumagai, M. Wolf, V. García-López, P.-T. Chiang, J. M. Tour and L. Grill, *ACS Nano*, 2016, **10**, 10945.
- 140 R. Eelkema, M. M. Pollard, J. Vicario, N. Katsonis, B. S. Ramon, C. W. M. Bastiaansen, D. J. Broer and B. L. Feringa, *Nature*, 2006, **440**, 163.
- 141 M. M. Green, M. P. Reidy, R. D. Johnson, G. Darling, D. J. O'Leary and G. Willson, *J. Am. Chem. Soc.*, 1989, **111**, 6452.
- 142 J. Berná, D. A. Leigh, M. Lubomska, S. M. Mendoza, E. M. Pérez, P. Rudolf, G. Teobaldi and F. Zerbetto, *Nat. Mater.*, 2005, **4**, 704.
- 143 A. Altieri, G. Bottari, F. Dehez, D. A. Leigh, J. K. Y. Wong and F. Zerbetto, *Angew. Chem. Int. Ed.*, 2003, **42**, 2296.
- 144 Q. Li, G. Fuks, E. Moulin, M. Maaloum, M. Rawiso, I. Kulic, J. T. Foy and N. Giuseppone, *Nat. Nanotechnol.*, 2015, **10**, 161.
- 145 Huisgen, *Proc. Chem. Soc.*, 1961, 357.
- 146 R. Feynman, *Eng. Sci.*, 1960, **23**, 22–36.